Neural Computing and Applications (2024) 36:7923–7952
https://doi.org/10.1007/s00521-024-09485-5

ORIGINAL ARTICLE

# Robust generation expansion planning in power grids under renewable energy penetration via honey badger algorithm

Adel A. Abou El-Ela[1] · Ragab A. El-Sehiemy[2] · Abdullah M. Shaheen[3] · Ayman S. Shalaby[4] · Mohamed T. Mouwafi[1]

Received: 13 August 2022 / Accepted: 14 January 2024 / Published online: 23 February 2024


## Abstract

Robust reliability Generation Expansion Planning (GEP) turns out to be a crucial step for an efficient energy management system in a modern power grid, especially under renewable energy employment. The integration of all such components in a GEP model makes it a large-scale, nonlinear, and mixed-variable mathematical modeling problem. In this paper, the presence of wind energy uncertainty is analyzed. Both long and short-term uncertainties are incorporated into the proposed GEP model. The first step concerns the impact of long-term wind uncertainties through the annual variations of the capacity credit of two real sites in Egypt at Zafaranh and Shark El-ouinate. The second step deals with the short-term uncertainties of each wind site. The wind speed uncertainty of each wind site is modeled by probability distribution function. Then, wind power is estimated from the wind power curve for each wind site and Monte-Carlo Simulation is performed. Fast Gas Turbine and/or Pump Hydro Storage are incorporated to cope with short-term uncertainties. Sensitivity analysis is implemented for 3, 6, and 12 stages as short and long planning horizons to minimize the total costs with wind energy penetration and emission reduction over planning horizons. Also, a novel Honey Badger Algorithm (HBA) with model modifications such as Virtual Mapping Procedure, Penalty Factor Approach, and the Modified of Intelligent Initial Population Generation is utilized for solving the proposed GEP problem. The obtained results are compared with other algorithms to ensure the superior performance of the proposed HBA. According to the results of the applicable test systems, the proposed HBA performs better than the others, with percentage reductions over CSA, AO, BES, and PSO ranging up to 4.2, 2.72, 2.7, and 3.4%, respectively.

**Keywords** Emission reduction constraint · Honey badger algorithm · Monte-Carlo simulation · Reliability constrained generation expansion planning · Virtual mapping procedure · Wind uncertainties

**List of symbols**

| | |
|---|---|
| $i$ | Discount rate |
| $K$ | Added unit in stage $t$ which are selected of different technologies |
| $N$ | Number of selected candidate units of technology $k$ |
| $u_t$ | Capacity vector of all candidate unit types in the stage |
| $t_o$ | Number of years between the reference date for discounting and the first year of study |
| $s$ | Number of years in each stage $t$ |
| $CI_k$ | Investment cost of each new candidate unit $k$ added in stage $t$ |
| $SV(u_t)$ | Salvage value cost |
| EENS | Expected energy not served |
| $O(X_t)$ | Expected energy not served cost |

✉ Ragab A. El-Sehiemy
elsehiemy@eng.kfs.edu.eg

[1] Electrical Engineering Department, Faculty of Engineering, Menoufiya University, Shebeen El-Kom 32511, Egypt

[2] Electrical Engineering Department, Faculty of Engineering, Kafrelsheikh University, Kafr El-Shaikh 33516, Egypt

[3] Department of Electrical Engineering, Faculty of Engineering, Suez University, Suez 43221, Egypt

[4] Middle Delta Electricity Production Company (MDEPCo), Talkha, Mansoura, Egypt

| | |
|---|---|
| $\delta_{k,t}$ | Salvage factor of unit $k$ added in stage $t$ |
| $T$ | Number of stages in the planning horizon |
| $X_t$, $G_{t,k}$ | The capacity and the expected energy produced for all existing and selected candidate units of each type $k$ |
| $\mathrm{FOM}_k$, $\mathrm{VOM}_k$ | Fixed and variable operating and maintenance costs |
| CEENS | Cost of EENS in \$/MWh |
| $\lambda$ | Percent reduction in total emission from the base case |
| $V$ | Wind speed |
| $x_i$ | Honey badger position |
| $\mathrm{lb}_i$, $\mathrm{ub}_i$ | Lower and upper limits of each position in the search space |
| $r_1, r_2, r_3, r_4, r_5, r_6, r_7$ | A random number between 0 and 1 |
| $S$ | Source strength |
| $d_i$ | Distance between $x_{\mathrm{prey}}$ prey and $i$th badger position |
| $\mathrm{iter}_{\max}$ | Maximum iterations number |
| Ch | Constant equal to 2 |
| $\beta$ | Ability of the honey badger to get food which is greater than or equal to 1 (default = 6) |
| $\breve{T}$ | Number of hours |
| LOLE | Loss of load expectation |
| IC | Total installed capacity |
| LP | Peak load |
| $E_i$ | Expected energy produced of the $i$th generator |
| $p_i$ | Availability of the $i$th generator |
| $U_i$ | Sum of capacities from 1st to $i$th generator |
| $\mathrm{in}v_{\mathrm{add}}$, $\mathrm{oper}_{\mathrm{add}}$, $\mathrm{fix}_{\mathrm{add}}$, and $S_{\mathrm{add}}$ | Investment, salvage, fixed and operation costs of FGT and PHS generating units |
| EEF | Equivalent energy function |
| PDF | Probability distribution function |
| MCS | Monte-Carlo Simulation |
| $X_{t,k}$ | Total capacity of existence and new units |
| $U_{\max,t}$ | Maximum construction number of each generation type at stage $t$ |
| $\mathrm{LD}_t$ | Peak load in stage $t$ |
| $X_{t,j}$ | Capacity of fuel type $j$ in stage $t$ |
| $\mathrm{SR}_{\min}$, $\mathrm{SR}_{\max}$ | Minimum and maximum required reserve capacity in stage $t$ |
| $\varepsilon$ | Maximum reliability criteria |
| LOLP | Loss of load probability |
| ELDC | Effective load distribution curve |
| CF | Capacity factor |
| $v_i$, $v_{\mathrm{r}}$, $v_{\mathrm{o}}$ | Cut-in, rated, and cut-out wind speeds |
| $K$, $C$ | Shape and scale Weibull parameter |
| $\mathrm{FR}^j_{\min}$, $\mathrm{FR}^j_{\max}$ | Lower and upper bounds of $j$th fuel type mix ratio in stage $t$ |
| $X_{t,w}$ | Wind output power of each wind site |
| $\mathrm{em}_j$ | Emission coefficient |
| $c$ | Discrete step size of the load |
| $Y_w$ | State of wind site penetration in stage $t$ |
| $\mathrm{LD}_{\mathrm{e}}$ | Effective load |
| $\mathrm{LD}_{\mathrm{d}}$ | Original load |
| $\mathrm{LD}_{oi}$ | Probabilistic load caused by the forced outage of the $i$th generator. |
| $q_i$ | FOR of the $i$th generator |
| $\mathrm{TC}_i$ | Objective function modified by PFA of $i$th individual |
| $\mathrm{Ob}_i$ | Objective function value without addition penalty factors for any constraints |
| $\omega$ | Penalty factor for the constraints validated |
| $p_1, p_2, p_3, p_4, p_5$ | Violation amounts of the constraint of spinning reserve margin; fuel mix ratio, LOLP, wind penetration level, and emission reduction, respectively |
| $a_1$, $a_2$, $a_3$ and $a_4$ | Polynomial coefficients using polyfit function in MATLAB |
| $x_i$ | Honey badger position |
| VMP | Virtual mapping procedure |
| MIIPG | Modified of intelligent initial population generation |
| $\mathrm{CAP}_{\min,t}$, $\mathrm{CAP}_{\max,t}$ | Minimum and maximum required capacities for a stage $t$ |

| | |
|---|---|
| $CAP_{\min,t-1}, CAP_{\max,t-1}$ | Minimum and maximum capacities in the previous stage |
| PFA | Penalty factor approach |
| $TC_i$ | Objective function modified by PFA of $i$th individual |
| PHS | Pump hydro storage |
| $Ob_i$ | Objective function value without additional penalty factors |
| FGT | Fast gas turbine |

# 1 Introduction

## 1.1 Motivation and main concepts

Generation Expansion Planning (GEP) is one of the most relevant problems in the planning of electric energy systems. It addressed the problem of identifying the most adequate technology, expansion size, sitting, and timing for the construction of new plant capacity considering economic criteria and technical power system constraints. However, it is necessary to guarantee that demands will be continuously supplied in all conditions were either an unexpected peak demand is occurred or an important unit fails [1]. The expansion planning criteria can be considered as conditions and limitations based on the decision-making process [2]. They are reflections of the positive features, which the planners would like to have in any future plan [3, 4] and preparing preventive control actions for active power [5] and reactive power issues [6].

Recently, the inclusion of uncertainties with various aspects has been considered in the GEP model as an effective approach to energy efficiency, conservations, $CO_2$ emission and environmental concerns. Thus, the planning should be investigated to affect by changing in parameters due to uncertainties and its capability to accommodate any changes [7]. In general, uncertainty analysis is critical for assessing the risks of any system that contains any type of uncertainty. The uncertainty which depends on nondeterministic in nature cannot be reduced while the uncertainty, which caused by limited knowledge about the system, is reduced as the search space expands [8]. However, integrating high share Renewable Energy Sources (RESs) within the power system planning had imposed a significant impact of uncertainties. Therefore, ignoring the variability and stochastic nature of RES within the GEP model may result in a lack of robustness of the planning results. Due to the fluctuation and the unpredictable characteristics of wind speed, wind power will have significant impact on the system security, stability, and reliability [9]. Therefore, techniques and approaches for dealing with such wind uncertainties should be more efficient and accurate which can be classified as probabilistic and possibilistic approaches [10]. Besides wind power uncertainty, there are other uncertainty sources such as load growth, fuel price, fuel costs, and the outage of generating units have also impact on expansion plans. Moreover, there are several studies considering wind energy penetration and PV as renewable sources for microgrid system such as [11, 12].

## 1.2 Literature review

In the planning process, the nature of the GEP problem is nonlinear, mixed-integer, highly constrained, and dynamic. The study of GEP without considering RESs has been introduced such as [13, 14] based on minimizing the total costs and satisfying reliability constraints. In recent years, several studies have been conducted on the reflection of environmental protection by adding emission limit constraints. Also, the impact of integrated RESs in power systems and their resulting uncertainties has been treated in the modeling of GEP problem. Expansion capacity planning requires not only total costs minimization, but also wind power uncertainty analysis and emission control should be handled over the planning horizon [15, 16].

The GEP problem has been solved by several analytical and optimization techniques without considering uncertainty analysis such as a Non-dominated Sorting Genetic Algorithm version II (NSGA-II), Modified Shuffled Frog Leaping Algorithm (MSFLA) that have been used in Refs. [14, 18 and 17], respectively. Also, Loss Of Load Probability (LOLP) has been computed as a reliability criterion in GEP problem which is evaluated based on the cumulative method as [19] where it has been modeled as Mixed Integer Programming (MIP). As a result, a model of least cost generation capacity expansion to control carbon dioxide emissions was presented, taking into account the effects of uncertain load and wind power generation [20, 21]. Moreover, the generation and transmission expansion planning (TEP) has been addressed without considering RESs uncertainty as [22]. The GEP dimensionality is large which the length of a string is equal to the product of the number of planning stages and the number of candidate unit's types. So that, the Virtual Mapping Procedure (VMP), Penalty Factor Approach (PFA), and the Modified of Intelligent Initial Population Generation (MIIPG) have been accomplished to decrease the GEP problem search space and reduce the computational time [17, 23].

In addition to the above, RES uncertainty is incorporated into generation and transmission expansion planning for a long and short-term planning horizon. In [24], the GEP problem with a certain penetration level of RESs has been solved by dynamic programming, while the wind and solar plants was modeled in Wein Automatic System Planning (WASP-IV).Besides, the effect of renewable energy uncertainties was assessed in the reliability and stability of power system. So that, it is important to develop decision support tools to help generation companies for achieving maximum their profit in a deregulated electricity market as [25, 26]. Also, a coordinated generation and transmission expansion planning in a deregulated electricity market have been addressed with wind power uncertainty analysis as [27]. The wind farm uncertainty was modeled by a normal PDF, and MCS has been utilized to include the uncertainty into the GEP or GEP/TEP problem. The combined GEP and TEP were handled with correlation of load and generation uncertainties that system uncertainties have been modeled with PDF and MCS to generate different random scenarios [28]. Also, Particle Swarm Optimizer (PSO) has been used to solve the TEP problem with reactive power planning and consideration of wind and load uncertainties as [29] while SFLA was performed in [30]. MCS was utilized to simulate the wind output power based on its PDF. Also, a deep learning method is one of the recent methods to deal with time series data such as the long short-term memory (LSTM) network algorithm which have been used for the same problems as in [31, 32]. But it has more steps to create output and consume more time which is not effective for expansion planning. However, the wind power uncertainty has been represented by annual variation of capacity factor based on historical data of wind location where the effect of wind power variation is analyzed at a certain probability of expectation [33]. Furthermore, both long and short-term wind power uncertainties were modeled within the GEP problem. The annual variation of the capacity credit was used to simulate the wind power long-term uncertainty. On the other side, the short-term uncertainty was simulated based on the hourly variation of wind power as [34]. Added to that, reserve margin has been adopted to cope with the uncertainty effect [34], while additional capacities of Pump Hydro Storage (PHS) and Fast Gas Turbine (FGT) have been utilized to cope with short-term uncertainty problems [35]. The problem of short-term uncertainty was modeled using the autoregressive moving average model. The main shortage in [33–35] is that the forced outage rate (FOR) of generating units was not taken into account at variable cost calculations where the FOR constitutes serious impacts on energy supplied of each generating units and reliability indies.

Furthermore, different battery technologies and demand side management options have been used to cope with the renewable energy uncertainties for off-grid hybrid renewable energy systems [36]. In this paper, the PV and biomass as renewable energy sources have been considered but the wind energy, which has more intermittent and variability of output power and affect the cycling charge of batteries, was not considered. However, the wind energy penetration in microgrid system design is considered in [37, 38], but it was dispatched as a certain value and wind energy uncertainty, and variability was not taken into account that has big effect on the system reliability. Furthermore, For the optimal sizing and techno-economic assessment of the intended hybrid microgrid system consist of solar diesel generator, PV, battery storage, and wind turbine, four dispatch approaches have been unitized: load following, generator order, combined dispatch, and cycle charging strategy while the system reliability study were carried out using Dig-SILENT Power Factory [39, 40]. Also, uncertainty of wind energy was not considered through system reliability calculation. Moreover, the wind speed and power conversions uncertainties are ignored in [41] and the wind power is calculated by specified model not based on a wind site study.

For reliability indies and variable cost calculations, the probabilistic production cost simulation using the Equivalent Energy Function (EEF) [14, 42] and Effective Load Distribution Curve (ELDC) [43] methods shows suitable accuracy with small computational time. Moreover, the RES uncertainties have been handled by the point estimate method for yearly peak loads uncertainties [44] and for distributed GEP in power distribution networks [45]. In [46, 47], the uncertainty of wind power has been modeled as a constraint depending on the wind availability in each hour. Therefore, the adoption of an hourly commitment of generating unit was considered to show the short-term impacts of long-term strategies through the decision-making process. In [15], the GEP analysis with different electricity scenarios for a mixed hydro-thermal and wind plants was performed which have impact in terms of costs and $CO^2$ emissions over the planning period. The carbon emissions have been added as an objective function as in [48].

Considering the incorporation of RESs into GEP problem, a whale optimization algorithm was carried out with adjustment strategies to decrease the GEP problem search space such as MIIGP, VMP, and PFA [49]. However, wind and solar output power have been studied at certain scenarios of penetration and emission reduction levels. In [50], differential evolution algorithm was used for minimizing the least cost GEP with certain penetration levels of wind capacity with emission reduction with certain penetration levels of solar power plants as [51, 52]. Also, wind power

was considered at only specific capacities through the modeling of GEP problem without discussing varied scenarios [53]. However, there are several wind scenarios which are not considered to lead to negative impact in reliability and security system.

### 1.3 Research gap and main contribution

RESs uncertainty consideration has a vital role in the planning and operation analysis of power system. Uncertainty analysis has an impact on the reliability and stability of the power system. So that, it is necessary, integrating the RES uncertainty analysis into the expansion planning problems. The presence of wind energy uncertainties is incorporated into the proposed GEP model in this paper. The first step is to assess the impact of long-term wind uncertainties using annual variations in capacity credit at two real-world sites in Egypt, Zafaranh and Shark El-ouinate. The second step addresses each wind site's short-term uncertainties. A PDF is used to model the wind speed uncertainty at each wind site. The wind power curve for each wind site is then used to estimate wind power, and MCS is performed. Sensitivity analysis is used for three, six, and twelve stages as short and long planning horizons to reduce total costs associated with wind energy penetration and emission reduction constraints over planning horizons.

The contributions of this paper can be summarized as follows:

- A robust multi-stage reliability constrained GEP model with wind power uncertainty and emission reduction is proposed to minimize the total costs under satisfaction constraints.
- The wind power is modeled by a PDF and MCS to simulate their accompanied uncertainties into the GEP model where two real wind sites with different mean and variance wind speeds are simulated.
- PHS and FGT are proposed to cope with the impact of short-term uncertainty.
- ELDC as a probabilistic production simulation (PPS) method is utilized to calculate the reliability indies and variable costs.
- The GEP results are analyzed at different reserve margins.
- A novel HBA with adjustable strategies of VMP, PFA, and MIIPG is proposed to achieve optimal and robust expansion planning.

### 1.4 Paper structure

The following portions of this work are organized as follows: Section II presents the conventional GEP model, whereas Section III establishes the proposed GEP model including the wind power uncertainty. Section IV describes the developed HBA for reliability constrained dynamic GEP. Section V defines the discussions and simulation findings. Finally, section VI concludes this paper.

## 2 Conventional GEP model

The Conventional GEP model as base case study can be formulated [14, 17, and 49] as follows:

### 2.1 Objective function

The objective function of the GEP problem is to minimize total costs over the planning period. In this context, the candidate units are responsible for the investment and salvage costs, but the candidate and existing units are jointly responsible for the operation, maintenance, and outage expenses.

Capital investment cost ($I(u_t)$) is the cost of purchasing new candidate units that can be provided by

$$I(u_t) = (1+i)^{-\mathrm{tc}} \times \sum_{k=1}^{N} \left(CI_k \times u_{t,k}\right) \tag{1}$$

$$\mathrm{tc} = t_o + s \times (t-1) \tag{2}$$

- *Salvage value cost* $\mathrm{SV}(u_t)$ is the actual cost of producing a unit at a specific time, considering the depreciation rate, which is determined as follows:

$$\mathrm{SV}(u_t) = (1+i)^{-Ts} \times \sum_{k=1}^{N} \left(\delta_{k,t} \times \mathrm{CI}_k \times u_{t,k}\right) \tag{3}$$

$$Ts = t_o + s \times T \tag{4}$$

The investment cost for a candidate unit chosen by the expansion plan is assumed at the start of the stage when it enters service. The salvage value, on the other hand, is determined at the conclusion of the planning horizon [54].

- *Operating and maintenance cost* $(\mathrm{M}(\mathrm{X_t}))$ is the operational and maintenance costs for existing and new candidate units which is assumed to occur in the middle of the corresponding planning stage as follows:

$$M(X_t) = \sum_{y=0}^{s-1} \left[ (1+i)^{-(tc+0.5+y)} \times \sum_{k=1}^{N} \left[ \mathrm{FOM}_k \times X_{t,k} + \mathrm{VOM}_k \times G_{t,k} \right] \right] \tag{5}$$

Each generation unit's fixed cost is determined by its capacity, and its variable cost is determined by the anticipated amount of energy that each generation unit will produce at each stage. Therefore, good prediction of the variable costs and reliability indies is essential to provide more precise estimation of the predicted energy produced by each generation unit.

Based on the expected energy not served (EENS), it is possible to calculate the anticipated energy generated by each generation unit. The EENS and LOLP, which are reliability indies, can be calculated by conventional method or PPS method to obtain cost modeling. The established capacity outage probability table, load probability table, and margin between them are the components of the traditional technique, which is used to compute reliability indies [55]. Because of the generous size of the GEP problem, this conventional method is not suitable and takes more computational time. Thus, there are other PPS methods that are more efficient for estimating the variable costs and the reliability indies with smaller computational time. In this context, the EEF method is one of PPS methods, but it depends on the greatest common factor for all adding capacities of existing and candidate units [42, 49]. Also, the ELDC is another method for any additional capacity in the planning [43].

- Expected energy not served (EENS) cost

  The EENS reflects an important reliability status in electrical power systems where customer satisfaction with continuous supply will influence the utility's competitive ability. Thence, continuous energy supply, which indicates better system reliability, can achieve customer satisfaction. However, depending on its FOR, any generating unit might not be available at any given time. As a cost term, EENS should be minimized because it cannot be made zero. This can be stated as follows:

$$O(X_t) = \sum_{y=0}^{s-1} [(1+i)^{-(\mathrm{tc}+0.5+y)} \times \mathrm{EENS}_t \times \mathrm{CEENS}] \tag{6}$$

  As a result, finding the best expansion planning is comparable to finding the objective function for solving the reliability restricted GEP problem as follows:

$$\mathrm{Ob} = \sum_{t=1}^{T} [I(u_t) + M(X_t) + O(X_t) - \mathrm{SV}(u_t)] \tag{7}$$

## 2.2 Constraints

- Upper construction limit ($u_t$): the quantity of all technology that has committed to meeting the stage t maximum construction number is as follows:

$$0 \le u_t \le U_{\max,t} \tag{8}$$

- Spinning reserve constrain (SR)t: The existing and new selected candidate units must meet the predicted load demand and capacity reserve margin limitation, which is represented as follows:

$$(1+\mathrm{SR}_{\min}) \times \mathrm{LD}_t \le \sum_{k=1}^{N} X_{t,k} \le (1+\mathrm{SR}_{\max}) \times LD_t \tag{9}$$

- *Fuel mix ratio*: The capacity of all the existing units must be limited when choosing candidate technology for expansion planning as follows:

$$\mathrm{FR}_{\min}^{j} \le \frac{X_{t,j}}{\sum_{k=1}^{N} X_{t,k}} \le \mathrm{FR}_{\max}^{j} \tag{10}$$

*Reliability constraint (LOLP)*: To continue supplying electricity continuously, both the new and current units need to meet the reliability criterion. A reliability metric called Loss of Load Probability (LOLP) is typically used to show how robust a system is in the face of unforeseen events.

$$\mathrm{LOLP}(X_t) \le \varepsilon \tag{11}$$

## 2.3 Effective load distribution curve (ELDC)

The calculation of expected energy produced by each generation unit, and reliability indices are especially critical issues for solving the GEP problem. For that purpose, PPS methods have been widely used for such calculations. The ELDC is used in this study for LOLP, and EENS calculation. Then, expected energy produced is calculated based on EENS calculation [43]. In the ELDC, the capacity and FOR of the generator $i$ are equivalent to $c_i$ and 0 with the fictitious load added to the original load. The sum of the original load and the probabilistic additional load is called effective load as formulated as:

$$\mathrm{LD}_e = \mathrm{LD}_d + \sum_{i=1}^{N} \mathrm{LD}_{\mathrm{oi}} \tag{12}$$

The ELDC is described in Fig. 1 can be calculated as:

$$\Phi_i(\mathrm{LD}_e) = \int \Phi_{i-1}(\mathrm{LD}_e - \mathrm{LD}_{\mathrm{oi}}) f_{\mathrm{oi}}(\mathrm{LD}_{\mathrm{oi}}) \mathrm{dLD}_{\mathrm{oi}} \tag{13}$$

where $\Phi_1(\mathrm{LD}_e)$ is the PDF of the ELDC convolved with the

PDFs of the outage capacities of the generators, 1st to $i$th;$\Phi_{i-1}(\mathrm{LD}_e - \mathrm{LD}_{\mathrm{oi}})$ is the PDF of the ELDC convolved with the PDFs of the outage capacities of all the generator, 1st to N-1. Also,$f_{\mathrm{oi}}(\mathrm{LD}_{\mathrm{oi}})$ is the PDF of the outage capacity of the $i$th generator. The ELDC can be generated by convolving the load curve and the plant outage capacity which leads to the following:

$$\acute{P}_n(x) = (1 - q_i)P_n(x) + q_i P_n(x - c) \tag{14}$$

Using the $\Phi_N(x)$, LOLE and EENS can be calculated using ELDC as following:

$$\mathrm{EENS} = \int_{\mathrm{IC}}^{\mathrm{IC+LP}} \Phi_N(x)\mathrm{d}x = \sum_{x=\mathrm{IC}}^{x=\mathrm{IC+LP}} \underset{n}{P}(x) \tag{15}$$

$$\mathrm{EENS} = \int_{\mathrm{IC}}^{\mathrm{IC+LP}} \Phi_N(x)\mathrm{d}x = \sum_{x=\mathrm{IC}}^{x=\mathrm{IC+LP}} \acute{P}(x) \tag{16}$$

The expected energy produced $E_i$ of the $i$th generator can be derived as follows:

$$E_i = T\,p_i \int_{U_{i-1}}^{U_i} \Phi_{i-1}(\mathrm{LD})\mathrm{dLD} \tag{17}$$

The probabilistic generated energy $\Delta E_i$ of the $i$th generator can be calculated as following:

$$\Delta E_i = \mathrm{EENS}_{i-1} - \mathrm{EENS}_i \tag{18}$$

## 3 Proposed GEP model including wind power uncertainty

The impacts of long and short-term wind power uncertainties are considered in the proposed robust GEP model. The long-term uncertainty is represented based on the wind capacity credit of each wind site which achieves the expansion constraints. Also, the short-term uncertainty is tackled by the MCS model.

### 3.1 Proposed GEP considering wind energy long-term uncertainty

Long-term uncertainty of the wind power is embedded into the planning model through the variation of the wind capacity credit of each site. The reliability indices such as LOLP and EENS are calculated based on existing and candidate units by PPS methods. FOR of wind plants are calculated, in this study, by sliding window technique as [49, 50]. It is assumed that FOR values for wind energy are constant over the study period. Based on that technique, the capacity factor of each wind site is estimated by annual wind energy produced divided by the rated capacity. The capacity factor is calculated using Weibull distribution parameters of wind speed [35] which is different for each wind site as follows:

$$\mathrm{CF} = \left[ \frac{e^{-\left(\frac{v_i}{C}\right)^K} - e^{-\left(\frac{v_r}{C}\right)^K}}{\left(\frac{v_r}{C}\right)^K - \left(\frac{v_i}{C}\right)^K} - e^{-\left(\frac{v_o}{C}\right)^K} \right] \tag{19}$$

However, the FOR values for wind plant of each site are calculated as follows:

$$\mathrm{FOR} = 1 - CF \tag{20}$$

The output of a wind site is related to the output of a single wind turbine, and it scales linearly with the number of wind generators. All wind turbines have similar input–output characteristics since installing different wind turbines in the same wind site is not usual.

Consequently, the wind power from two Egyptian wind sites (Zafaranh and Shark El-Ouinate) is added to candidate units in the base case. The long-term uncertainty of the wind power is imposed into the planning model through the variation of the wind capacity credit of each site. The traditional objective function of GEP model described in Eq. (7) is updated by adding the costs of investment in$v_w$, operating oper$_w$, and fixed fix$_w$ terms of each wind site as follows:

$$\mathrm{ob}_{\mathrm{long}} = \mathrm{ob} + \mathrm{ob}_w \tag{21}$$

$$\mathrm{ob}_w = \mathrm{in}v_w + \mathrm{oper}_w + \mathrm{fix}_w - S_w \tag{22}$$

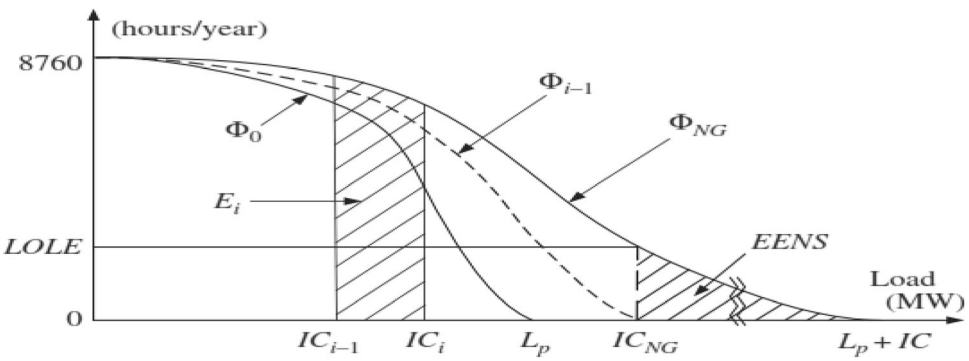


**Fig. 1** Reliability indices and ELDC

Also, additional constraints related to the two wind sites should be merged which are the wind level penetration and emission reduction constraints over all planning period as follows:

$$0.1 \times \sum X_{t,k} \leq \sum_{t=1}^{T} \sum_{w=1}^{2} X_{t,w} \leq 0.2 \times \sum X_{t,k} \tag{23}$$

$$\sum X_{t,w} > 0 \tag{24}$$

$$\sum_{t=1}^{T} \sum_{j=1}^{N} (X_{t,j}(j) \times \mathrm{em}_j) < \lambda \tag{25}$$

For ease of the construction and manpower, two wind sites should not be selected in the same stage which is represented in the following constraint:

$$\sum_{w=1}^{2} Y_w \leq 1 \tag{26}$$

### 3.2 Proposed GEP considering wind energy short-term uncertainty

The MCS is used to include wind short-term uncertainty in the problem. Each site of Zafaranh and Shark El-ouinate has different mean and variance wind speed which affect the output capacity of it. Therefore, Weibull distribution parameters are assessed individually for each site. Moreover, there are two main sources of uncertainties related to wind RESs: wind speed forecast uncertainty and the wind-electrical power conversion curve [8]. The wind speed uncertainty is simulated by accurate estimation of Weibull parameters, while the wind speed power conversion curve is selected based on each wind site characteristics. The scenario-based MCS is a commonly used tool to deal with wind speed uncertainty in the problem [56]. For each scenario of MCS, the wind speed is a randomly generated based on its Weibull PDF which is characterized by the following equation [57, 58]:

$$f(v) = \left(\frac{K}{C}\right)\left(\frac{v}{C}\right)^{K-1} \exp\left(-\left(\frac{v}{C}\right)^{K}\right) \tag{27}$$

where $v$ is the wind speed.

The most efficient model for each site is applied based on the minimum error of energy density for Zafaranh $g_z(v)$ and Shark El-ouinate $g_s(v)$ sites, respectively [59] as follows:

$$g_z(v) = \left(\frac{v - v_i}{v_r - v_i}\right)^2 \tag{28}$$

$$g_s(v) = a_1 v^3 + a_2 v^2 + a_3 v + a_4 \tag{29}$$

The general form can be represented as the following equation:

$$p(v) = \begin{cases} p_r & v_r \leq v \leq v_o \\ p_r * g(v) & v_i \leq v \leq v_r \\ 0 & \text{otherwise} \end{cases} \tag{30}$$

The objective function of the proposed GEP model with short-term uncertainty ($\mathrm{ob}_{\mathrm{sc}}$) is defined as adding the costs of adding units ($\mathrm{ob}_{\mathrm{add}_{\mathrm{cap}}}$) to the base case (ob) and wind costs ($\mathrm{ob}_w$) as follows:

$$\mathrm{ob}_{\mathrm{sc}} = \mathrm{ob}_{\mathrm{long}} + \mathrm{ob}_{\mathrm{add}_{\mathrm{cap}}} \tag{31}$$

$$\mathrm{ob}_{\mathrm{add}} = \mathrm{inv}_{\mathrm{add}} + \mathrm{oper}_{\mathrm{add}} + \mathrm{fix}_{\mathrm{add}} - \mathrm{S}_{\mathrm{add}} \tag{32}$$

For each scenario, all constraints for the base case and long-term uncertainty are examined. The addition of new FGT and/or PHS units under a wind power violation scenario could alter the system's fuel mix ratio Eq. (10) and overall emission Eq. (25). Therefore, whenever a new unit is added, those constraints need to be checked again.

## 4 Developed HBA for reliability constrained dynamic GEP Problem

### 4.1 Honey badger algorithm

HBA is an entirely novel meta-heuristic technique that is based on how honey badgers hunt for their prey in an intelligent way. It is brave and prefers to spend time alone in self-made burrows, only meeting other badgers to mate. To access bird nests and beehives for food, it can also climb trees. A honey badger finds its prey through sniffing, digging, or following a honey guide bird, which can find beehives but cannot obtain honey. Exploration and exploitation phases are developed from the honey badger's dynamic search behavior using digging and honey-finding methods [60]. Firstly, an initial population is generated based on the number of honey badger and their respective positions as follows:

$$x_i = \mathrm{lb}_i + r_1 \times (\mathrm{ub}_i - \mathrm{lb}_i) \tag{33}$$

The intensity ($\mathrm{In}_i$), which is related to concentration, prey strength, and the distance between the prey and the honey badger, is then specified. The motion of the prey will be fast at high smell intensity and vice versa. The intensity is defined as follows:

$$\mathrm{In}_i = r_2 \times \frac{S}{4\pi d_i^2} \tag{34}$$

$$S = (x_i - x_{i+1})^2 \tag{35}$$

$$d_i = x_{\mathrm{prey}} - x_i \tag{36}$$

The density factor ($\alpha$) is specified and updated which controls time varying randomization to ensure a smooth transition from exploration to exploitation phase. So that, this factor decreases with iterations to decrease randomization with time as follows:

$$\alpha = \mathrm{Ch} \times \exp\left(\frac{-t}{\mathrm{iter}_{\max}}\right) \tag{37}$$

A flag ($F$), which alters the search direction, is generated to enhance escaping from local to optima regions. The positions of the agents are then updated, and $x_{new}$ is modified in accordance with the two stages of the digging phase and the honey phase as follows:

$$F = \begin{cases} 1 & \text{if } r_3 \leq 0.5 \\ -1 & \text{otherwise} \end{cases} \tag{38}$$

Then, the positions of agent's $x_{new}$ are updated via digging and honey phases A. The honey badger's digging phase resembles the shape of a cardioid, which can be simulated by doing the following:

$$x_{\mathrm{new}} = x_{\mathrm{prey}} + F \times \beta \times I \times x_{\mathrm{prey}} + F \times r_4 \times \alpha \times d_i \times |\cos(2\pi r_5) \times [1 - \cos(2\pi r_6)]| \tag{39}$$

where $\beta$ is the ability of the honey badger to get food which is greater than or equal to 1 (default = 6).

In the honey phase, a honey badger follows the honey guide bird to reach beehive which is simulated as follows:

$$x_{\mathrm{new}} = x_{\mathrm{prey}} + F \times r_7 \times \alpha \times d_i \tag{40}$$

The flowchart diagram of the HBA is shown in Fig. 2. Therefore, a honey badger performs search closed to prey location, and the searching process is influenced by time varying ($\alpha$). Also, the HBA performance is significantly affected by two user-defined parameters ($\beta and Ch$) so that these parameter values should be selected carefully. In this context, the best parameter values ($\beta = 6, \text{and} \mathrm{Ch} = 2$) of the proposed algorithm are taken from [60].

B. *Enhanced HBA for the proposed large-scale GEP model.*

The proposed GEP problem is a high large dimensional problem with multiple conflicting objectives, uncertainty analysis and nonlinear constraints which represents a complex optimization problem. Thus, some modifications are proposed to enhance the HBA to deal with this problem. VMP, PFA, and MIIPG improve the effectiveness of the meta-heuristic algorithm as follows [23, 49]:

(1) VMP

This step aims to transform each combination of candidate units into a dummy variable which represents a position of each agent in the search space. Thus, the decision variable of each stage is represented by single variable only which needs less memory space. Further, if the mapped variable took part in all related solutions, a slight change in the mapped variable will reduce the infeasible solutions. Thus, a multivariable could be mapped into a single variable, which is the decision variable in this problem. As five diverse types of units are assumed to be decision variables for each stage, the array size of the problem solution is increased by multiples of 5.

(2) MIIPG

Generation of initial population is incorporated to decrease the search space and improve performance of heuristic algorithm. Thus, the minimum and maximum cumulative capacity is assumed to be available in the previous stages. Consequently, the minimum and maximum required capacity for each stage can be calculated based on reserve margin as follows:

$$\mathrm{CAP}_{\min,t} = (1 + \mathrm{SR}_{\min}) \times \mathrm{LD}_t - \mathrm{CAP}_{\min,t-1} \tag{41}$$

$$\mathrm{CAP}_{\max,t} = (1 + \mathrm{SR}_{\max}) \times \mathrm{LD}_t - \mathrm{CAP}_{\max,t-1} \tag{42}$$

where$\mathrm{CAP}_{\min,t}$ and $\mathrm{CAP}_{\max,t}$ are the minimum and maximum required capacities for a stage $t$ which are based on forecasted load demand and reserve margin; $\mathrm{CAP}_{\min,t-1}$ and $\mathrm{CAP}_{\max,t-1}$ are minimum and maximum capacities in the previous stage which are the sum of capacities of existence and selected units. Their values are always updated with each selected candidate combination.

Figure 2 shows the flowchart illustrating the detail of the proposed robust expansion model with long-term uncertainty representation. According to block (A), the constraints (8–11) are checked for each particle. Then, the infeasible particles are penalized as in block (B) while the wind short-term uncertainty is studied for feasible solutions only as in block (C). For each feasible particle in the population, by using the MCS, the wind speed is randomly generated based on it is a Weibull PDF. Then, the output power for each wind site is calculated based on the power curve for each site. For each wind power scenario, the reserve, fuel mix ratio and reliability constraints are checked. If any constraint is violated, additional capacities are added to cope with wind energy short-term uncertainty effects.

The wind capacity credit from each wind site is considered trough the wind long-term uncertainty analysis. Then for each feasible solution, the wind speed scenarios are generated based on PDF by MCS technique to deal with wind short-term uncertainty. The number of scenarios is 500 to model the uncertainties. The wind speed scenarios and

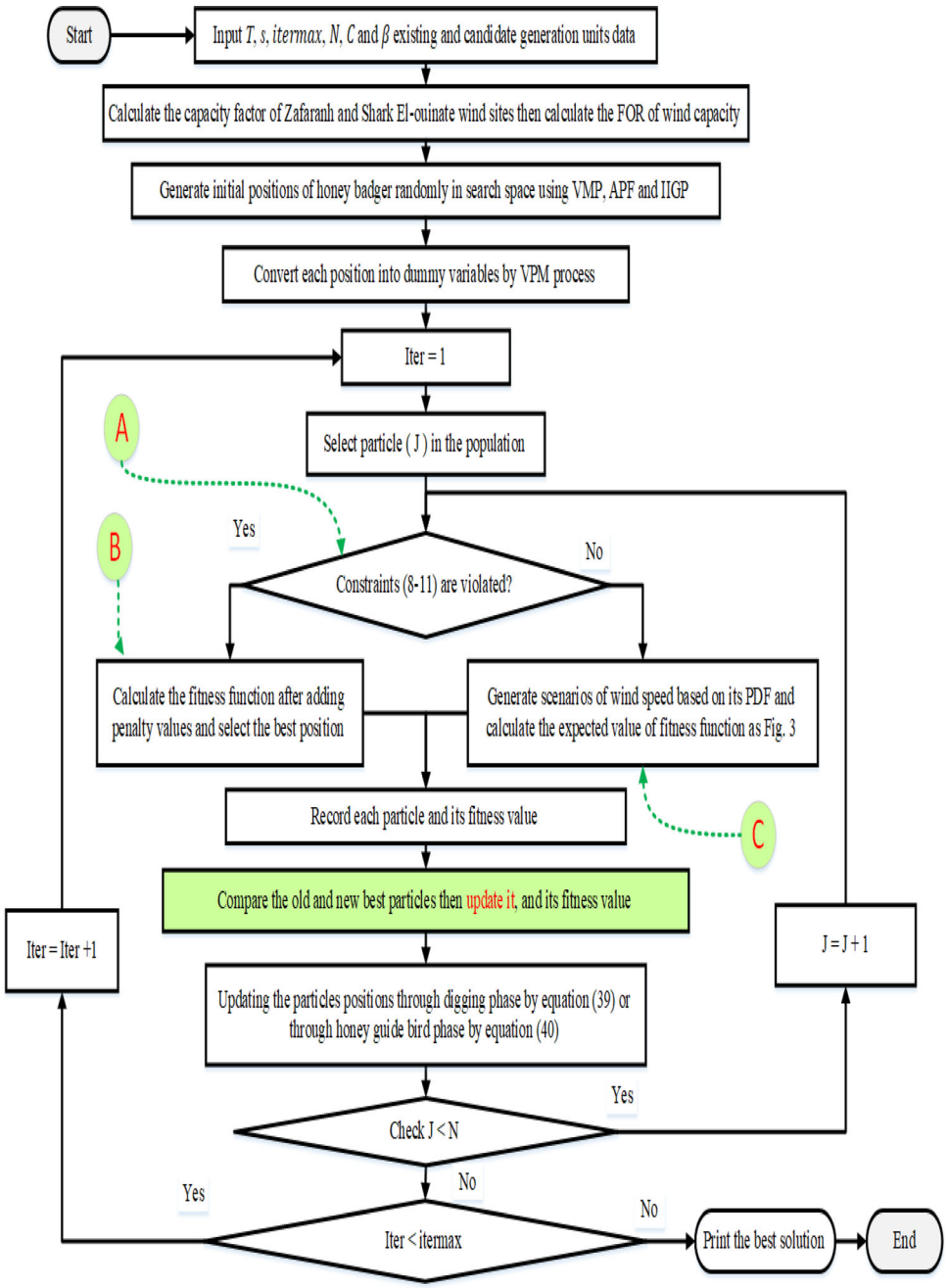


**Fig. 2** Flowchart for the proposed HBA for solving the GEP incorporating wind power uncertainty

constraints checked are established for any stage containing wind power penetration. But the constraints are only checked for stages that have no wind power with a mean value of wind power scenarios of previous stages. Moreover, the wind power for all previous stages is taken into account at current stage study as mean value of wind power scenarios. The constraints are checked for each scenario, and FGT and PHS units are used to adapt the scenarios violated constraints. The LOLP is used as a reliability criterion which calculated by ELDC. As LOLP value is proportional to reserve capacity over the planning horizon, the GEP with uncertain analysis is studied at different reserve margin. Then, the results of the wind uncertainty analysis, total expansion planning cost, and LOLP are compared.

(3) Modified objective function with PFA

The PFA can be used to convert a constrained problem into an unconstrained problem. As a result, the objective function is modified to include proportional penalty values for each violated constraint, avoiding the infeasible solutions in later iterations.

The total costs are given as the objective function with the PFA (TC):

$$\mathrm{TC}_i = \left[\mathrm{Ob}_i + \omega \times \left(\sum p_1 + \sum p_2 + p_3 + p_4 + p_5\right)\right] \quad (43)$$

Figure 3 describes the evaluation of the expected total costs with short-term uncertainty representation based on scenarios of MCS. As shown, each scenario is checked for the constraints and other generating units of PHS and/or FGT can be added as referred in block (D), in some cases, to meet the constraints. Then, the objective function of the current scenario is calculated, which is saved and MCS is reiterated. After convergence of MCS, the meaning of all expected values of scenarios is evaluated. For each scenario, the objective function is calculated after adding the costs due to addition capacities. Then, the mean value of all scenarios is considered as the objective function for this particle.

## 5 5 Simulation results

### 5.1 Test system description

The test system consists of 15 existing generation units (Oil, Liquid Natural Gas (LNG), coal and Nuclear) is tabulated in Table 1. Five different new generation technologies are selected as candidate conventional units (Oil, LNG, Coal, and Nuclear) as in Table 2. The forecasted peak load is illustrated in Table 3, with initial peak load of 5000 MW, and other data of existing and candidate generation units are taken from [14, 23, and 61]. In this study, the discount rate is taken 8.5%; LOLP criterion at each stage is considered of 0.01. The lower and upper limits for reserve margin are set at 20 and 50%, respectively. EENS cost is assumed to be 0.05 $/kWh. The bounds of capacity mixes by fuel types are 0% and 30% for oil-fired power plants, 0 and 40% for LNG-fired, 20 and 60% for coal-fired, and 30 and 60% for nuclear, respectively. The emission coefficient for oil is 0.85, LNG is 0.5, and coal is 1.05 while the reduction in total emission is considered as

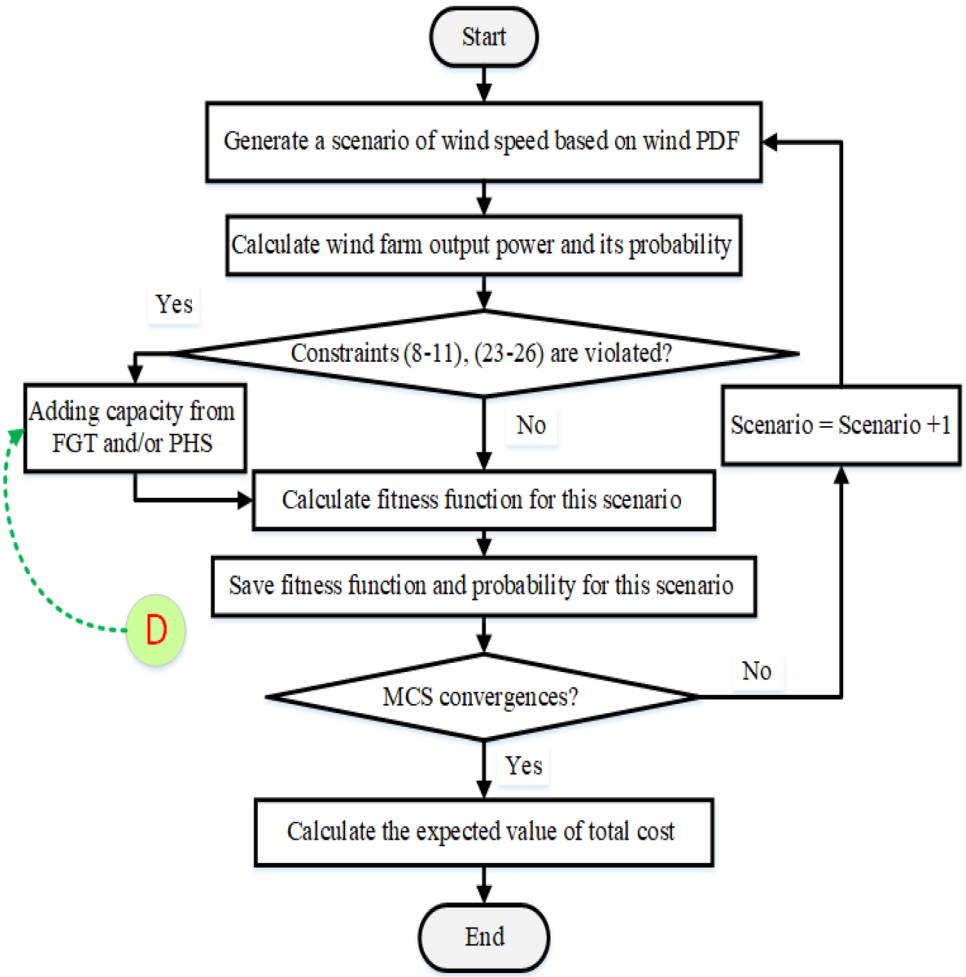


**Fig. 3** Evaluation of the expected total costs incorporating wind power short-term uncertainty

**Table 1** Technical and economic data of existing generating units

| Name | No. of units | Unit capacity (MW) | FOR% | Operating cost ($/kWh) | Fixed O&M cost ($/kW-Mon) |
|---|---|---|---|---|---|
| Oil#1 | 1 | 200 | 7.0 | 0.024 | 2.25 |
| Oil#2 | 1 | 200 | 6.8 | 0.027 | 2.25 |
| Oil#3 | 1 | 150 | 6.0 | 0.030 | 2.13 |
| LNG G/T #1 | 3 | 50 | 3.0 | 0.043 | 4.52 |
| LNG C/C #1 | 1 | 400 | 10.0 | 0.038 | 1.63 |
| LNG C/C #3 | 1 | 400 | 10.0 | 0.040 | 1.63 |
| LNG C/C #4 | 1 | 450 | 11.0 | 0.035 | 2.00 |
| Coal #1 | 2 | 250 | 15.0 | 0.023 | 6.65 |
| Coal #2 | 1 | 500 | 9.0 | 0.019 | 2.81 |
| Coal #3 | 1 | 500 | 8.5 | 0.015 | 2.81 |
| Nuclear #1 | 1 | 1000 | 9.0 | 0.005 | 4.94 |
| Nuclear #2 | 1 | 1000 | 8.8 | 0.005 | 4.63 |

**Table 2** Technical and economic data of candidate plants

| New units | $U_{max}$ | Capacity (MW) | FOR % | Operating cost ($/kWh) | Fixed O&M cost ($/kW-Mon) | Capital cost ($/kW) | Lifetime (yrs) |
|---|---|---|---|---|---|---|---|
| Oil | 5 | 200 | 7.0 | 0.021 | 2.20 | 812.5 | 25 |
| LNG C/C | 4 | 450 | 10.0 | 0.035 | 0.90 | 500.0 | 20 |
| Coal (bit) | 3 | 500 | 9.5 | 0.014 | 2.75 | 1062.5 | 25 |
| Nuclear #1 | 3 | 1000 | 9.0 | 0.004 | 4.60 | 1625.0 | 25 |
| Nuclear #2 | 3 | 700 | 7.0 | 0.003 | 5.50 | 1750.0 | 25 |
| FGT | 4 | 150 | 0.8 | $53.23*10^{-3}$ | 0.5725 | 71.474 | 25 |
| PHS | 3 | 200 | 5.0 | $0.227*10^{-3}$ | 0.4363 | 154.377 | 50 |

**Table 3** Forecasted peak demand in Gwatts

| Stage | 1 | 2 | 3 | 4 | 5 | 6 | 7 | 8 | 9 | 10 | 11 | 12 |
|---|---|---|---|---|---|---|---|---|---|---|---|---|
| | 7 | 9 | 10 | 12 | 13 | 14 | 15 | 17 | 18 | 20 | 22 | 24 |

10% of base case [49, 50, and 62]. The cost of unserved energy, or EENS, which is calculated by ELDC method, is set at 0.05 $/kWh. The initial period is set as two years while the economic and technical characteristics of the additional units are listed in Table 2 as [35].

The candidate wind sites, in this study, are Zafranah, and Shark El-ouinate wind farm sites. The first site, Zafaranh wind farm, is in the Suez Gulf which is approximately 200 km southeast Cairo. While the second site, Shark El-ouinate, is in depth southern Egyptian desert. The operational data of wind turbines and their descriptive statistics, which are considered in this study for the two sites, are recorded in Table 4. Added to that, the time series data of the wind speed for the year 2019 in hourly basis of Zafranah, and Shark El-ouinate wind farm sites are taken from [63]. As shown in Table 4, the mean wind speed value of Zafaranh site is greater than its value for Shark El-ouinate site. But the variance and standard deviation for Zafaranh site are less than it values for Shark El-ouinate. Thus, most values of the generated wind speed scenarios based on PDF for Zafaranh site will be around the corresponding mean and below its maximum speed other than Shark El-ouinate site which reaches maximum speed values with a smaller number of scenarios. So, studying each wind site with its characteristics is especially important for the reliability, and security of the power system.

## 5.2 GEP results and discussion

HBA is used to solve the GEP problem as base case and wind energy uncertainty analysis based on the considered three policies planning horizon as follows:

**Table 4** Candidate wind turbine characteristics

| Site | Zafranah | Shark El-ouinat |
|---|---|---|
| Wind turbine type | Nordex N43 | Nordex-N100 |
| Rated power ($P_r$) (kw) | 600 | 2500 |
| Hub height (m) | 55 | 100 |
| Cut-in wind speed (m/s) | 2.5 | 3 |
| Cut-off wind speed (m/s) | 25 | 25 |
| Rated wind speed (m/s) | 15 | 12.5 |
| Mean (m/s) | 7.1468 | 6.4966 |
| Maximum (m/s) | 15.897 | 13.508 |
| Minimum (m/s) | 1.8 | 0.077 |
| Standard deviation / Variance (m/s) | 1.8666 / 3.4844 | / 6.3198 |

- Policy-1: short-term GEP problems with 6-year planning horizon
- Policy-2: long-term GEP problems with 12-year horizon
- Policy-3: long-term GEP problems with 24-year horizon

Two cases are considered in the first two polices in this paper. The first case study is performed using the proposed framework, and results are compared with different other techniques in the literature. This case study is the base case in which the original problem is solved without wind energy penetration and emission reduction constraint. Then, the second case study is implemented for solving the GEP problem which includes wind energy uncertainty analysis and emission reduction objective function. Added to that, an extra scenario that aims at minimizing the total GHG emission as an objective function:

$$\min \text{GHG Emission} = \left( \sum_{t=1}^{T} \sum_{j=1}^{N} (X_{t,j}(j) \times \text{em}_j \right) \tag{41}$$

The long-term and short-term wind uncertainties are studied with 500 MCS scenarios of wind speed based on PDF of each wind site. Each planning horizon consists of two years of stage, making them to be 3, 6, and 12 stages in short- and long-term planning horizons. The number of years between the reference date of cost calculations and the first year of study ($t$) are assumed to be 2 years.

## 5.3 Policy-1: simulation results for 3-stages case study

### 5.3.1 GEP results as base case of 3-stages case study

For policy-1, as a base case study, the GEP model is solved, without considering wind energy penetration and emission reduction constraints, using different optimization techniques. The competitive techniques of Particle Swarm Optimization (PSO) [23], Crow Search Algorithm (CSA) [64], Aquila Optimizer (AO) [65], Blad Eagle Search (BES) [66], and the proposed HBA are carried out for solving the GEP. For all techniques, the specified parameters are 200 of iteration number, 60 of population size and 30 simulation runs while the population size is taken 30 for BES only since each individual per each iteration has two times for function evaluations. Moreover, the penalty factor value ($\omega$), which is used to penalize the infeasible solutions, is equal to $10^{15}$. PSO, CSA, AO, BES, and HBA are executed and their optimal results, and the associated statistical indices of each applied algorithm are recorded in Table 5. This table displays the total number of each type of power plant in the planning model for comparative algorithms.

The obtained comparative results show that the proposed HBA has achieved the best total costs compared to the other applied algorithms, whereas the improvement of the objective function is equal to 3.2, 1.1 and 0.081% in costs over the CSA, AO, and BES, respectively. Also, the proposed HBA provides the smallest standard error and deviation of $2.27*10^7$ and $1.25*10^7$, respectively. Moreover, the best cost of PSO and HBA are the same and the average cost of PSO is less than HBA, but HBA provides the smallest worst total cost with $7.1736*10^9$ $ where the CSA, AO, BES and PSO achieve $7.3464*10^9$, $7.3267*10^9$, $7.1976*10^9$ and $7.2265*10^9$ $, respectively. In the context, the HBA is more staple during transfer from run to another one as shown in Fig. 4. Also, the LOLP values are shown in Table 6 which indicates that the reliability criterion is satisfied for each applied algorithm. Moreover, Fig. 5 describes the convergence curves of CSA, AO, BES, PSO and the proposed HBA. It can be observed from Fig. 5 that the HBA algorithm shows better convergence rates compared to the others. As shown, it provides a higher convergence rate in finding the least objective in approximately 140 iterations.

**Table 5** Total Number of newly candidate units at each stage for case 1 and the related Descriptive statistics

| Algorithm | Candidate units | | | | | Descriptive statistics ($) | | | | |
|---|---|---|---|---|---|---|---|---|---|---|
| | Oil | LNG | Coal | Nuclear #1 | Nuclear #2 | Best cost $*10^9$ | Average cost $*10^9$ | Worst cost $*10^9$ | Standard error $*10^7$ | Standard dev. $*10^8$ |
| CSA | 6 | 5 | 4 | 3 | 0 | 6.7331 | 7.0613 | 7.3464 | 2.58 | 1.41 |
| AO | 3 | 8 | 3 | 3 | 0 | 6.5924 | 7.0511 | 7.3267 | 2.99 | 1.64 |
| BES | 1 | 9 | 3 | 3 | 0 | 6.5734 | 6.963 | 7.1976 | 2.53 | 1.38 |
| PSO | 1 | 8 | 3 | 3 | 0 | 6.5204 | 6.8125 | 7.2265 | 3.09 | 1.69 |
| HBA | 1 | 8 | 3 | 3 | 0 | 6.5204 | 6.856 | 7.1736 | 2.27 | 1.25 |

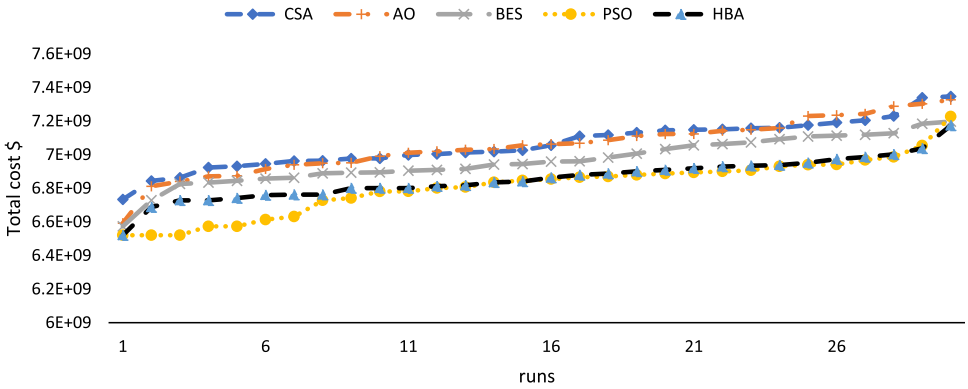


**Fig. 4** Recorded total cost characteristics of the competitive algorithms for policy 1

**Table 6** Values of LOLP criterion for policy 1-A

| Stages | CSA | AO | BES | PSO | HBA |
|---|---|---|---|---|---|
| 1 | 0.009787 | 0.009787 | 0.009787 | 0.009787 | 0.009787 |
| 2 | 0.00879 | 0.007991 | 0.005251 | 0.005251 | 0.005251 |
| 3 | 0.005648 | 0.00374 | 0.003686 | 0.008899 | 0.008899 |

### 5.3.2 GEP results considering wind energy uncertainty 3-stages case study

The previous base case for 3-stages GEP model is resolved considering wind energy long-term and short-term uncertainty analysis. While the emission reduction contraint is taken into account based on emission value in the base case. In this policy, a wind power plant source from two different wind sites are added as two wind plants to the

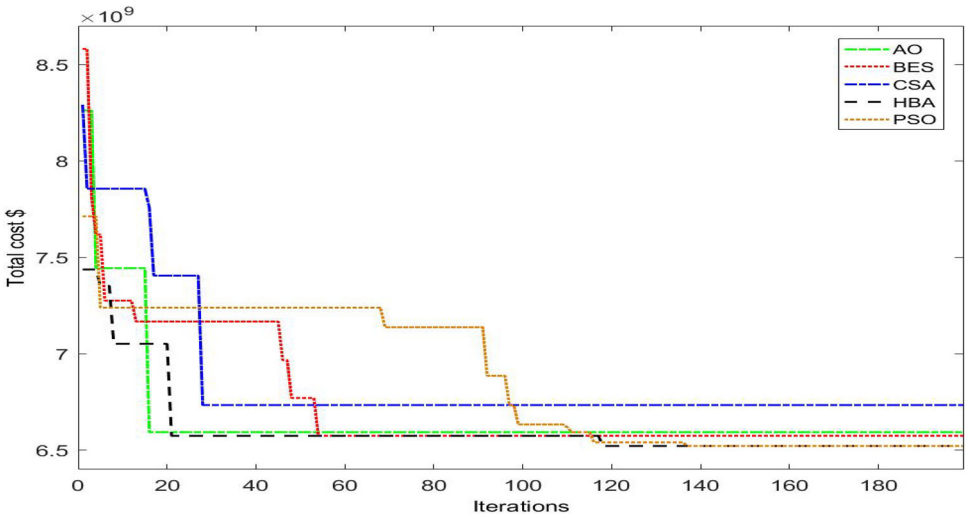


**Fig. 5** Converging characteristics of the competitive algorithms for policy 1

**Table 7** Number of newly candidate units for 50%and 60% reserve Margin

| Stages | Number of units at 50% Reserve | | | | | | | | | Number of units at 60% Reserve | | | | | | | | |
|---|---|---|---|---|---|---|---|---|---|---|---|---|---|---|---|---|---|---|
| | Oil | LNG | Coal | Nuclear #1 | Nuclear #2 | Wind (Zaf) | Wind (Shark) | FGT | PHS | Oil | LNG | Coal | Nuclear #1 | Nuclear #2 | Wind (Zaf) | Wind (Shark) | FGT | PHS |
| 1 | 2 | 1 | 3 | 2 | 0 | 0 | 1 | 1 | 1 | 2 | 2 | 2 | 2 | 1 | 0 | 1 | 0 | 0 |
| 2 | 2 | 1 | 0 | 1 | 1 | 1 | 0 | 0 | 0 | 0 | 0 | 0 | 1 | 0 | 0 | 1 | 2 | 3 |
| 3 | 0 | 0 | 0 | 0 | 0 | 0 | 1 | 1 | 2 | 0 | 0 | 1 | 0 | 0 | 1 | 0 | 2 | 1 |
| Total | 4 | 2 | 3 | 3 | 1 | 1 | 2 | 2 | 3 | 2 | 2 | 3 | 3 | 1 | 1 | 2 | 4 | 4 |

candidate units in the base case. The total wind contribution level is up to 10–20% of the installed capacity as an alternative candidate plant. Also, the emission reduction coefficient is taken as 10% reduction percent from the base case over the planning horizons. The proposed HBA are utilized while the penalty factor value ($\omega$) is equal to $10^{20}$. Table 7 summarizes the optimal results obtained for 50 and 60% two reserve capacity margin cases considering the wind speed scenarios by MCS via PDF for each feasible particle, as shown in Fig. 6. After generating wind speed scenarios based on its PDF, wind output power for each wind site is estimated for Zafaranhand Shark El-Ouinate site, respectively. Then, the reserve, fuel mix ratio, and LOLP constraints are checked for each scenario, and the total cost is calculated for scenarios which satisfy the constraints. When the particle with wind power scenario does not satisfy all constraints, the addition capacities of FGT and/or PHS are added to cope with wind power short-term uncertainty. Figure 7 shows the total costs for each scenario as example that are combines the costs of existing, candidate and addition units.

For scenarios which violate the constraints, the FGT and/or PHS are added until the constraints are satisfied and the economic effect is added to total costs of scenario. The total cost of the scenario is saved, and MCS is reiterated until the scenario's number is ended. The proposed HBA is applied for the two different specified levels of the reserve margin and the number of newly candidate technology type, FGT and PHS number units at each planning stage are tabulated in Table 7 at different reserve margin. The PDF and CDF of LOLP values of each scenario before and after adding the FGT and/or PHS units are shown in Fig. 8 as related to 50% reserve capacity and in Fig. 9 as related to 60% reserve capacity.

The PDF and CDF of LOLP values at each stage demonstrate the positive impacts of the FGT and/or PHS additional units on the reliability system target. At stage 1, as shown in Fig. 8A, the number of scenarios which satisfy the LOLP constraint is less than 40% of the total scenarios before adding FGT and/or PHS units. At the same stage, 100% of the scenarios satisfy the LOLP constraint after adding FGT and/or PHS units. On the other side, at stage 2, the values of LOLP criteria are achieved without any addition of FGT and/or PHS units as shown in Fig. 8B. Moreover, at wind penetration level constraints over the planning horizon, which mean wind power from previous stages are considered, no constraints are satisfied for all scenarios at the stage 3 without adding any capacity as shown in Fig. 8C. Because of the reliability criteria is affected by reserve capacity, the GEP with wind uncertainty analysis is solved at 60% maximum threshold of the reserve margin. As shown in Fig. 9A, all wind power scenarios achieve all the constraints without adding FGT

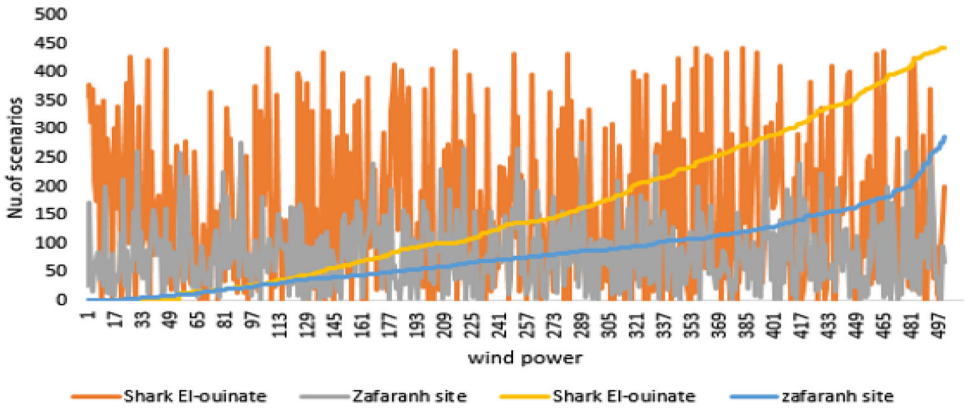


**Fig. 6** Example 500 scenarios of wind output power of each wind site

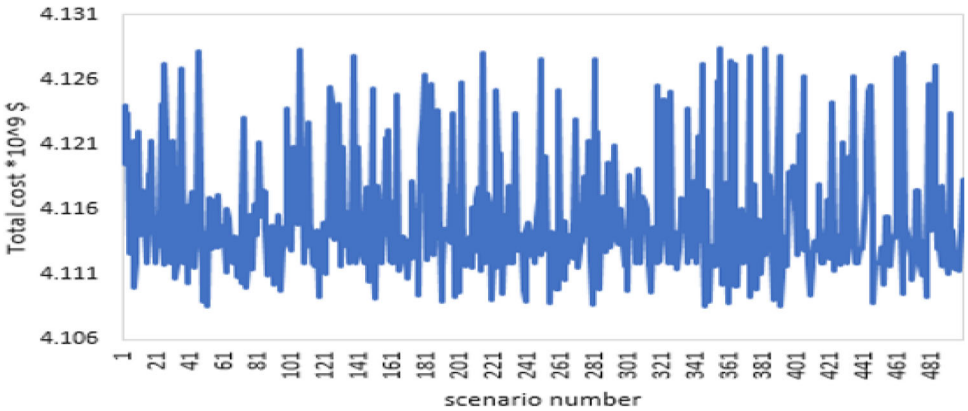


**Fig. 7** Expected costs of the generated scenarios of wind power in Fig. 5

and/or PHS units at stage 1. On contrary, adding capacities FGT and/or PHS units are required for stage 2 in order to achieve the reliability criteria where at increased wind penetration level as shown in Fig. 9B. Increasing the necessary reserve margin results in violating the LOLP constraint for many scenarios. Therfore, installing more units of FGT and/or PHS is required as illustrated in Fig. 9C at stage 3. Thus, the total cost of expansion planning is increased considering 60% reserve margin, which is $8.205*10^9$ $, which is higher than the case of 50% reserve margin, which is $8.183*10^9$ $.

## 5.4 Policy-2: Simulation results for 6 stages case study

### 5.4.1 GEP results as base case of 6 stages case study

In this policy, a long-term planning horizon of 12-year (6 stages) is managed. In the first case, wind penetration and emission reduction constraint are not included where the CSA, AO, BES, PSO, and the proposed HBA are employed. Their optimal results in terms of the total number of new conventional candidate generation units for each stage of the planning horizon and the accompanied statistical indices are recorded in Table 8.

From Table 8, it is found that the proposed HBA provides the minimum total costs and better performance than other algorithms. The proposed HBA has achieved a 2.5, 4.5, 2.5, and 5.16% enhancement in costs over CSA, AO, BES, and PSO, respectively. It should be noted that the performance of PSO algorithms is affected by the planning horizon than the others.

The proposed HBA derives the best performance over the other competitive algorithms since it achieves the least total costs of their best, average, worst, standard error, and standard deviation of $1.2996*10^{10}$, $1.3675*10^{10}$, $1.4211*10^{10}$, $4.43*10^7$ and $2.43*10^8$, respectively. Moreover, the recorded costs of the comparative algorithms indicate that the proposed HBA has smallest and stable values of the worst, average, and best of total costs over all runs as shown in Fig. 10. Also, the proposed HBA shows the best convergence rate compared to the others in finding the least objective target as displayed in Fig. 11.

### 5.4.2 GEP results considering wind energy uncertainty via 6 stages case study

In this case, the proposed HBA is utilized for solving the GEP problem at 50% and 60% reserve margin. The optimal results of the number of newly candidate technology type,

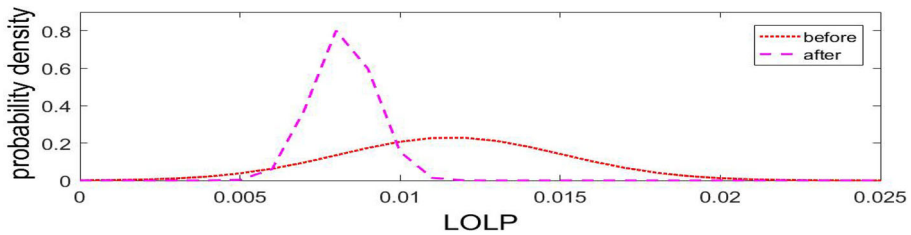


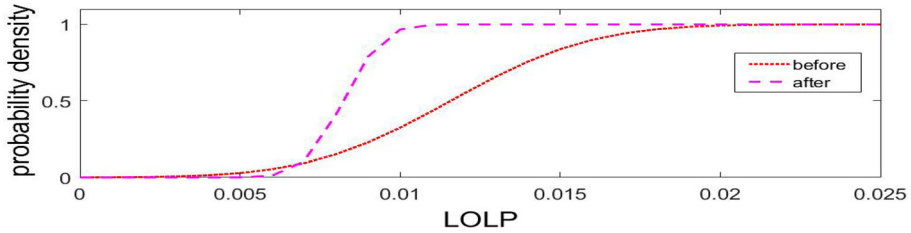


a. PDF and CDF of LOLP values for stage 1

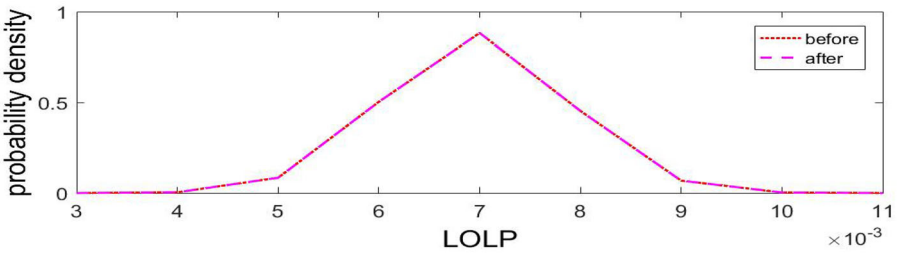


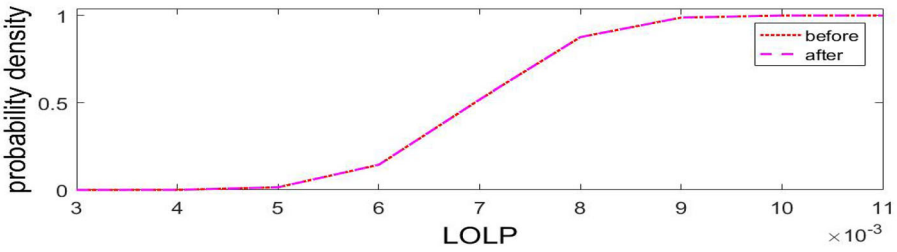


b. PDF and CDF of LOLP values for stage 2

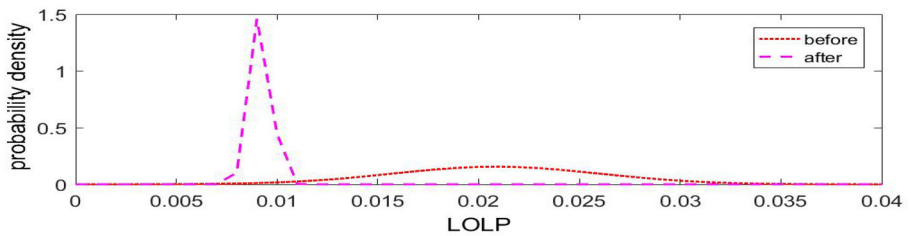


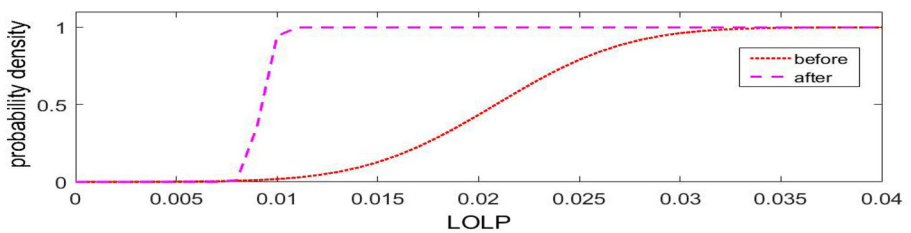


c. PDF and CDF of LOLP values for stage 3

**Fig. 8** PDF and CDF of LOLP values before and after adding FGT and/or PHS units at 50% reserve capacity

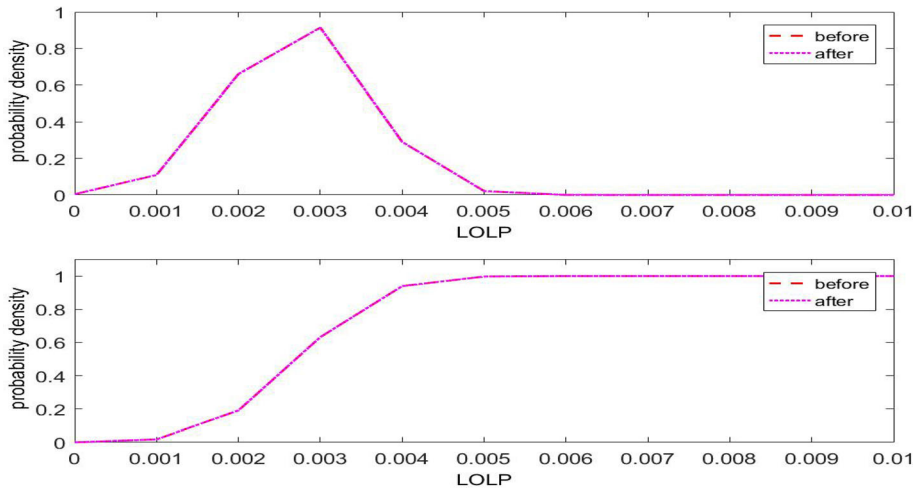


a. PDF and CDF of LOLP values for stage 1

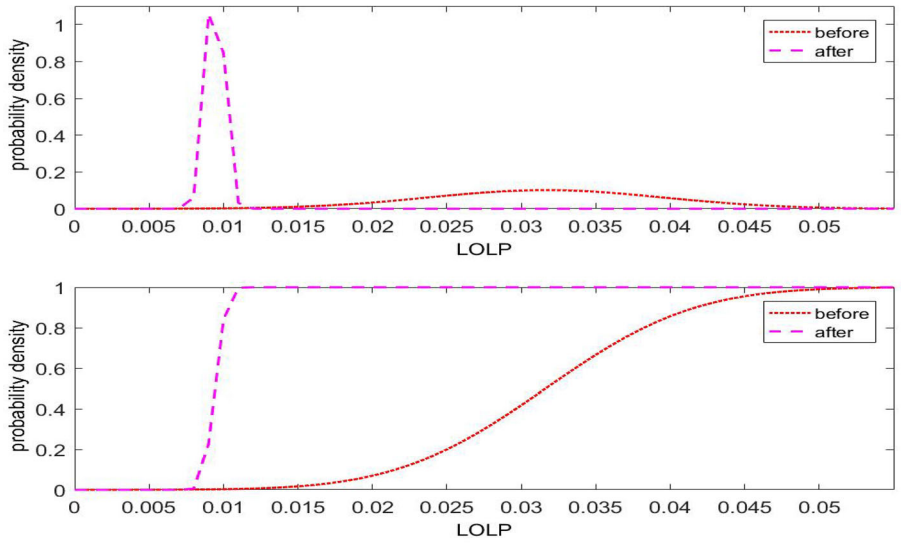


b. PDF and CDF of LOLP values for stage 2

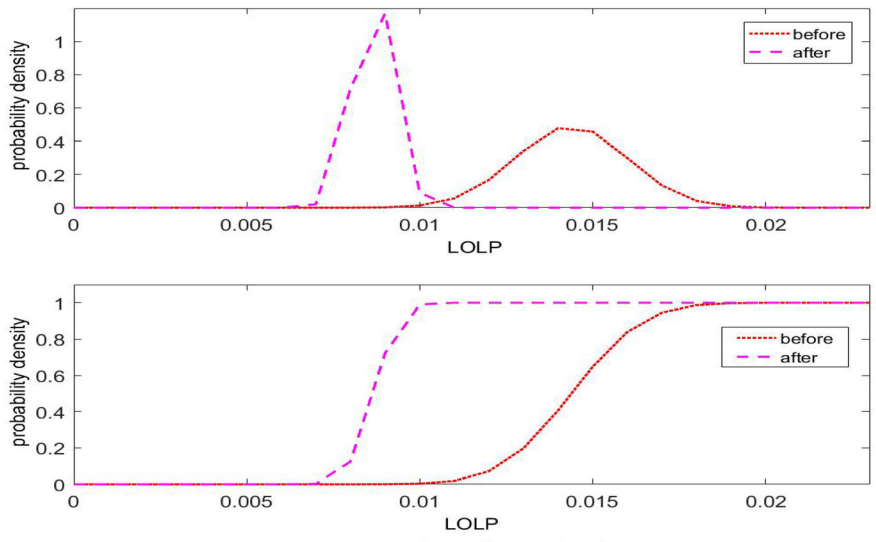


c. PDF and CDF of LOLP values for stage 3

**Fig. 9** PDF and CDF of LOLP values before and after adding FGT and/or PHS units at 60% reserve capacity

**Table 8** Total number of newly candidate units in each stage for the base case of policy 2 and the associated Statistical

| Algorithm | Candidate units | | | | | Statistical results | | | | |
|---|---|---|---|---|---|---|---|---|---|---|
| | Oil | LNG | Coal | Nuclear #1 | Nuclear #2 | Best cost $*10^{10}$ $ | Average cost $*10^{10}$ $ | Worst cost $*10^{10}$ $ | Standard error $*10^{7}$ $ | Standard dev. $*10^{8}$ $ |
| CSA | 8 | 11 | 6 | 4 | 0 | 1.3327 | 1.4306 | 1.445 | 6.42 | 3.51 |
| AO | 13 | 9 | 7 | 4 | 0 | 1.362 | 1.4473 | 1.5319 | 6.87 | 3.76 |
| BES | 14 | 10 | 5 | 4 | 0 | 1.3335 | 1.3982 | 1.4477 | 5.57 | 3.05 |
| PSO | 11 | 12 | 5 | 4 | 0 | 1.3702 | 1.4179 | 1.5179 | 6.32 | 3.46 |
| HBA | 5 | 13 | 6 | 4 | 0 | 1.2996 | 1.3675 | 1.4211 | 4.43 | 2.43 |

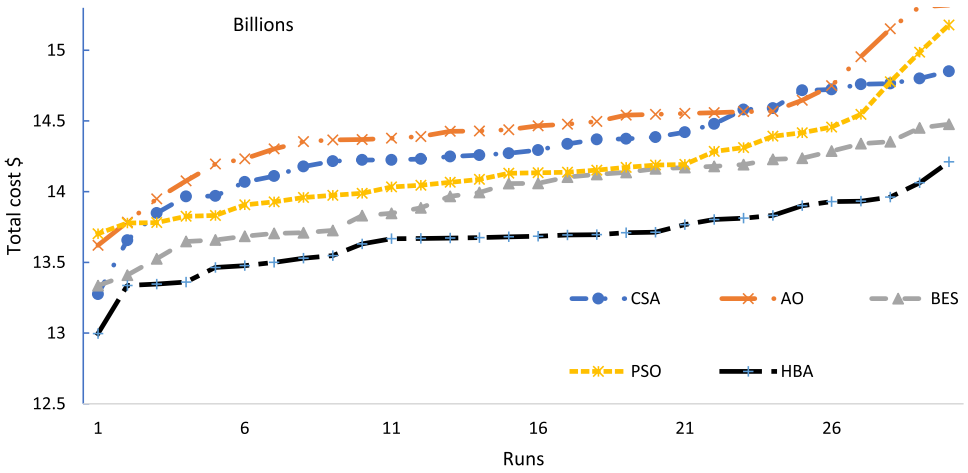


**Fig. 10** Recorded total cost characteristic of the competitive algorithms for policy 2

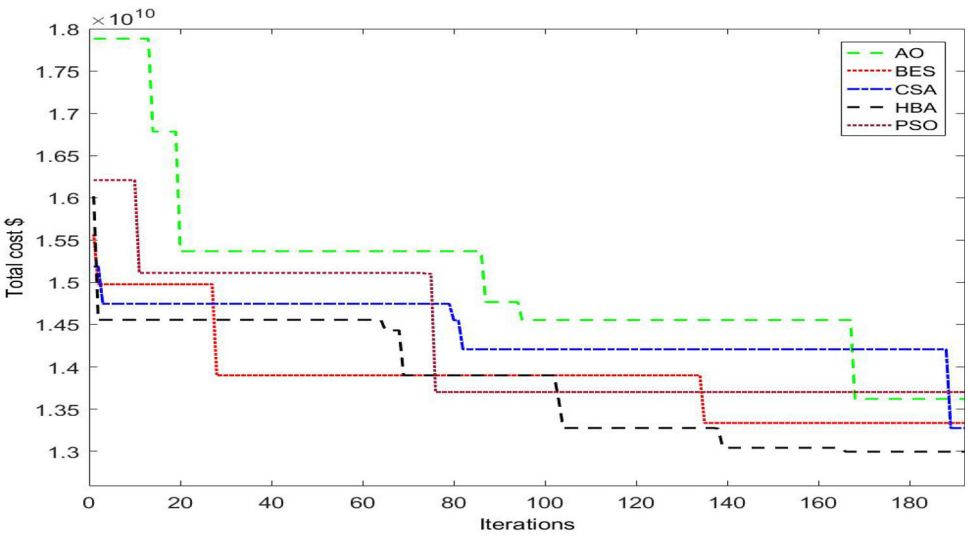


**Fig. 11** Converging characteristics of the competitive algorithms for policy 2

FGT and PHS number units at each planning stage are recorded in as shown in Table 9. As shown, the wind power is penetrated at 1, 2 and 6 stages for GEP model at 50% or 60% reserve margin.

In addition to that, the LOLP values are represented as PDF and CDF before and after adding capacities of FGT and/or PHS for stages 1, and 2 as shown in Fig. 12. As shown, the number of scenarios which satisfy the LOLP constraint is less than 40% of the total scenarios before adding FGT and/or PHS units. At the same stage, 100% of the scenarios satisfy the LOLP constraint after adding FGT and/or PHS units. At stage 2, the values of LOLP criteria

**Table 9** Number of newly candidate units at 50% (60%) reserve margin for policy 2-b

| Stages | Candidate units at 50% reserve margin | | | | | | | | | Candidate units at (60%) reserve margin | | | | | | | | |
|---|---|---|---|---|---|---|---|---|---|---|---|---|---|---|---|---|---|---|
| | Oil | LNG | Coal | Nuclear #1 | Nuclear #2 | Wind (Zaf) | Wind (Shark) | FGT | PHS | Oil | LNG | Coal | Nuclear #1 | Nuclear #2 | Wind (Zaf) | Wind (Shark) | FGT | PHS |
| 1 | 4 | 1 | 2 | 2 | 0 | 0 | 1 | 2 | 1 | 4 | 3 | 2 | 2 | 0 | 0 | 0 | 0 | 0 |
| 2 | 1 | 1 | 2 | 0 | 0 | 1 | 0 | 0 | 2 | 1 | 1 | 2 | 1 | 0 | 0 | 0 | 0 | 0 |
| 3 | 1 | 0 | 1 | 1 | 1 | 0 | 0 | 0 | 0 | 0 | 0 | 0 | 1 | 1 | 1 | 0 | 0 | 0 |
| 4 | 0 | 1 | 0 | 1 | 0 | 0 | 0 | 0 | 0 | 1 | 1 | 0 | 1 | 0 | 0 | 1 | 0 | 0 |
| 5 | 3 | 0 | 1 | 1 | 1 | 1 | 0 | 0 | 0 | 1 | 0 | 1 | 0 | 1 | 1 | 0 | 0 | 0 |
| 6 | 0 | 2 | 0 | 0 | 0 | 0 | 1 | 0 | 0 | 0 | 1 | 0 | 0 | 0 | 0 | 1 | 0 | 0 |
| Total | 9 | 5 | 6 | 5 | 2 | 2 | 2 | 2 | 3 | 7 | 6 | 6 | 5 | 2 | 2 | 2 | 0 | 0 |

are improved as well. At stage 3, there is no wind power penetration whereas the LOLP criterion is preserved at the mean value of wind power scenarios of the previous stages and additional units. At stage 4, no new wind power is installed. Despite the LOLP constraint is violated in this stage with 0.02 value, it is maintained to 0.005 after considering the previous additional units. Moreover, at stages 5, and 6, the wind power is added and checked the constraints with previous additional units; the LOLP criterion is guaranteed within the prescribed limit. Considering the constraint of the reserve margin at 60%, total planning costs and reliability criteria are affected which depend on the timing of wind power deployed.

The results of expansion planning at 60% reserve margin indicate that the wind power plants are deployed in later planning stages of 3, 4, 5 and 6, as shown in Table 9 where the LOLP values at stage 3 are displayed in Fig. 13. The constraints, especially reliability constraint, are not affected by wind power deployed in later stages and LOLP criterion is preserved inside the permissible limit and less than 0.01 without any additional capacities due to increase spinning reserve and wind power penetrated in the last stages. Even though no additional units are added, the total expansion planning costs at 50% reserve margin is less than it at 60% reserve margin which are $1.6017*10^{10}$, and $1.6665*10^{10}$, respectively.

#### 5.4.3 Policy- 3:Simulation results for 12 stages case study

GEP results as base case of 12 stages case study

In this policy, a long-term planning horizon 24-year (12 stages) is conducted. CSA, AO, BES, PSO, and the proposed HBA are employed for solving reliability constraint GEP for this policy. Table 14 shows the total number of new candidate generation units for each stage. Also, their achieved result in terms of the statistical indices of each applied algorithm is recorded in Table 10.

As shown, the proposed HBA has the best performance compared to the others with percentage reductions of 4.2, 2.72, 2.7, and 3.4% over CSA, AO, BES and PSO, respectively. Thus, the HBA achieves the optimum reliability constrained GEP with the minimum total cost. It achieves the least total costs of their best, average, worst, standard error, and standard deviation of $2.3706*10^{10}$, $2.4953*10^{10}$, $2.6569*10^{10}$, $1.33*10^{8}$ and $7.31*10^{8}$, respectively. The total cost results of each run of the comparative algorithms are drawn as displayed in Fig. 14 which indicates that the proposed HBA has the least statistical results compared to others. Also, the proposed HBA shows the best convergence rate compared to the others in finding the least objective target as displayed in Fig. 15. These figures show the fast response rate of the proposed HBA in reaching the most economical solutions.

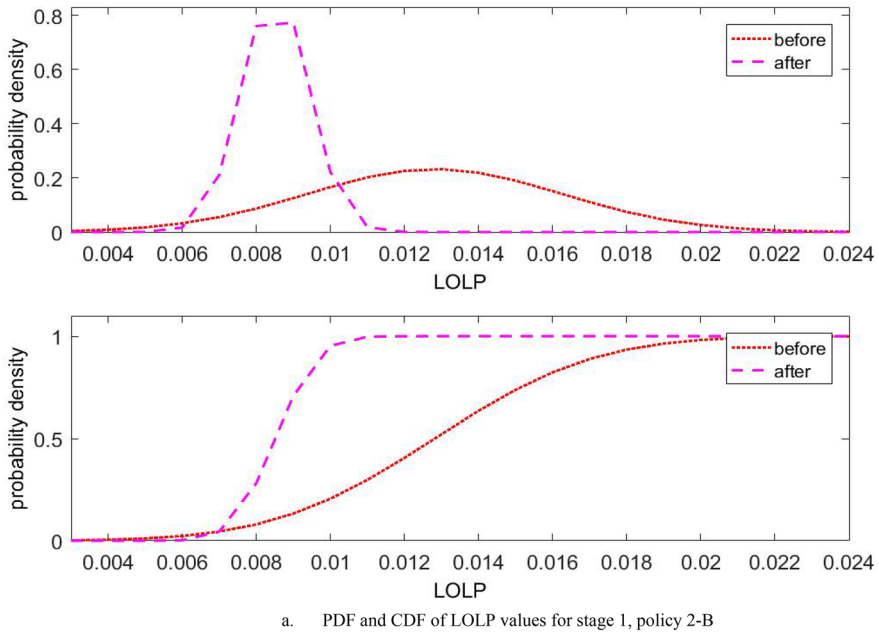


a. PDF and CDF of LOLP values for stage 1, policy 2-B

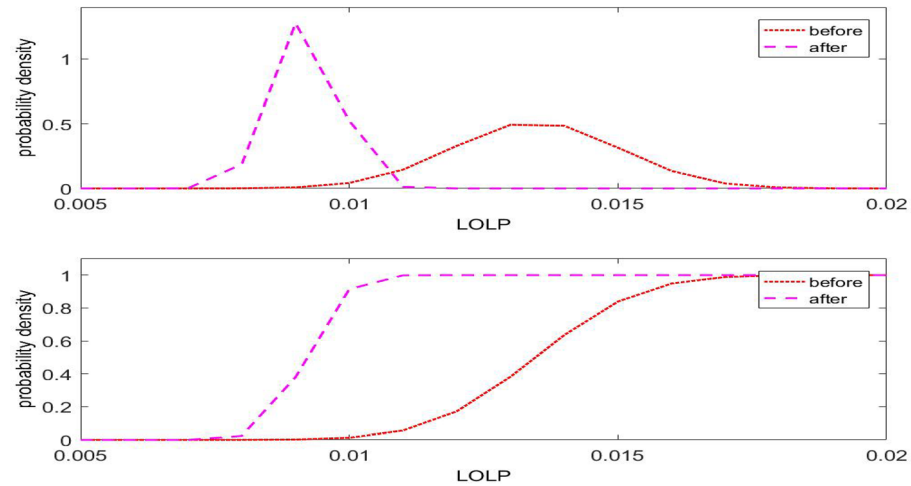


b. PDF and CDF of LOLP values for stage 2, policy 2-b

**Fig. 12** PDF and CDF of LOLP values before and after adding capacity at 50% reserve capacity

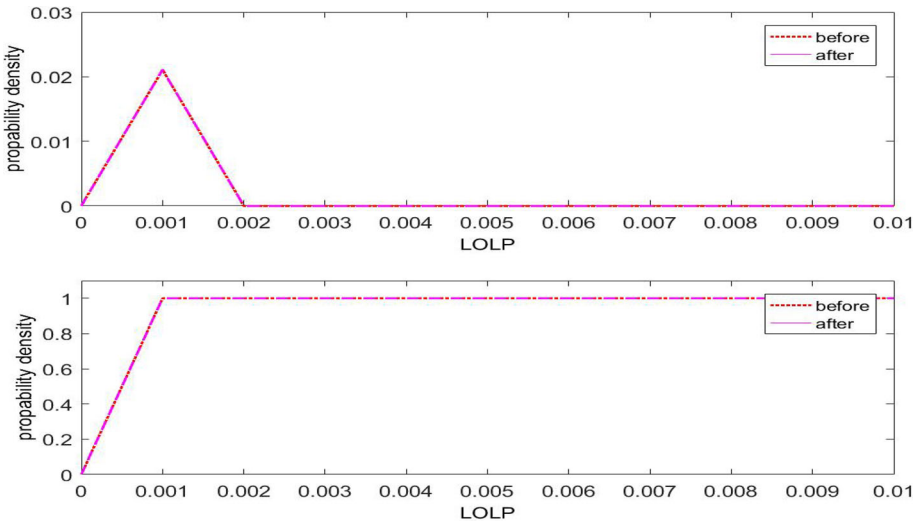


**Fig. 13** PDF and CDF of LOLP values before and after adding capacity at 60% reserve capacity

**Table 10** Total Number of newly candidate units in each stage for the base case of policy- 3-a

| Stages | Oil | LNG | Coal | Nuclear #1 | Nuclear #2 | Best cost $*10^{10}$ $ | Average cost $*10^{10}$ $ | Worst cost $*10^{10}$ $ | Standard error $*10^{8}$ $ | Standard dev. $*10^{8}$ $ |
|---|---|---|---|---|---|---|---|---|---|---|
| CSA | 21 | 19 | 12 | 9 | 3 | 2.4753 | 2.6369 | 2.8054 | 1.48 | 8.13 |
| AO | 18 | 17 | 18 | 9 | 0 | 2.4369 | 2.595 | 2.8125 | 1.86 | 10.2 |
| BES | 21 | 12 | 12 | 8 | 4 | 2.4366 | 2.5521 | 2.7434 | 1.34 | 7.35 |
| PSO | 16 | 20 | 14 | 9 | 3 | 2.4541 | 2.5687 | 2.7193 | 1.34 | 7.35 |
| HBA | 10 | 19 | 10 | 8 | 4 | 2.3706 | 2.4953 | 2.6569 | 1.33 | 7.31 |

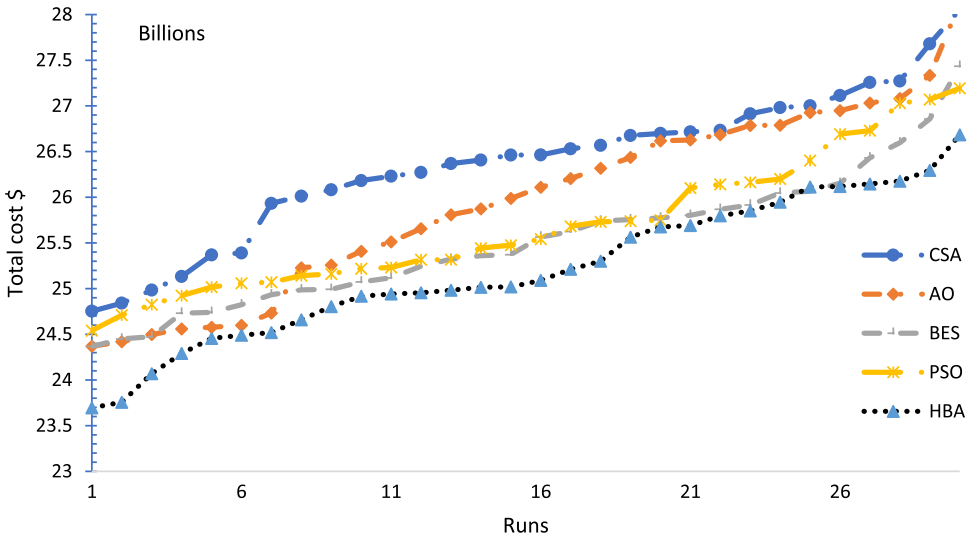


**Fig. 14** Recorded costs characteristics of the competitive algorithms for policy 3

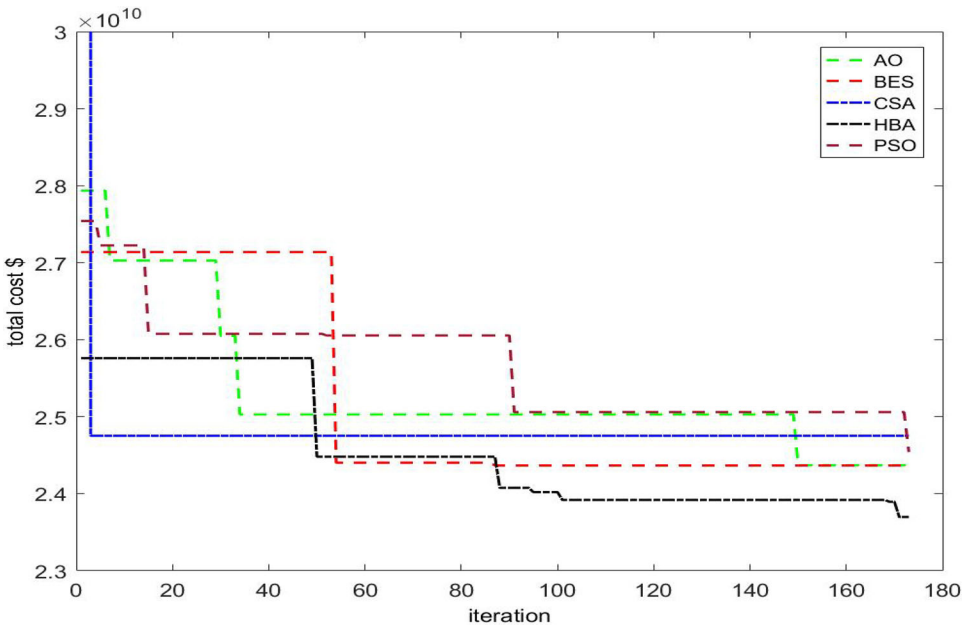


**Fig. 15** Converging rates of the competitive algorithms for policy 3

**Table 11** Total Number of newly candidate units at 50% (60%) reserve margin for policy 3-b

| Stages | Candidate units at 50% reserve margin | | | | | | | | | Candidate units at 60% reserve margin | | | | | | | | |
|---|---|---|---|---|---|---|---|---|---|---|---|---|---|---|---|---|---|---|
| | Oil | LNG | Coal | Nuclear #1 | Nuclear #2 | Wind (Zaf) | Wind (Shark) | FGT | PHS | Oil | LNG | Coal | Nuclear #1 | Nuclear #2 | Wind (Zaf) | Wind (Shark) | FGT | PHS |
| 1 | 0 | 0 | 3 | 3 | 0 | 0 | 1 | 1 | 1 | 0 | 0 | 3 | 3 | 0 | 0 | 1 | 1 | 1 |
| 2 | 0 | 1 | 2 | 0 | 0 | 0 | 1 | 3 | 2 | 1 | 1 | 0 | 1 | 1 | 1 | 0 | 0 | 0 |
| 3 | 2 | 1 | 0 | 0 | 0 | 1 | 0 | 0 | 0 | 2 | 0 | 1 | 0 | 0 | 0 | 1 | 0 | 0 |
| 4 | 0 | 2 | 2 | 1 | 0 | 0 | 1 | 0 | 0 | 1 | 2 | 1 | 2 | 0 | 0 | 1 | 0 | 0 |
| 5 | 0 | 0 | 1 | 1 | 0 | 0 | 0 | 0 | 0 | 2 | 0 | 0 | 0 | 0 | 1 | 0 | 0 | 0 |
| 6 | 0 | 0 | 0 | 0 | 2 | 1 | 0 | 0 | 0 | 1 | 0 | 3 | 0 | 0 | 1 | 0 | 0 | 0 |
| 7 | 0 | 0 | 0 | 1 | 0 | 1 | 0 | 0 | 0 | 1 | 0 | 0 | 1 | 0 | 0) | 1 | 0 | 0 |
| 8 | 1 | 1 | 2 | 0 | 0 | 0 | 1 | 0 | 0 | 2 | 0 | 0 | 0 | 2 | 1 | 0 | 0 | 0 |
| 9 | 0 | 0 | 0 | 0 | 0 | 1 | 0 | 1 | 0 | 0 | 1 | 0 | 0 | 1 | 0 | 0 | 0 | 0 |
| 10 | 1 | 0 | 1 | 2 | 0 | 0 | 1 | 0 | 0 | 2 | 0 | 0 | 0 | 0 | 0 | 1 | 4 | 3 |
| 11 | 1 | 1 | 0 | 2 | 1 | 0 | 0 | 0 | 0 | 1 | 1 | 2 | 0 | 0 | 0 | 0 | 0 | 0 |
| 12 | 0 | 1 | 0 | 1 | 1 | 0 | 0 | 0 | 0 | 0 | 1 | 1 | 1 | 0 | 0 | 1 | 4 | 3 |
| Total | 10 | 7 | 11 | 11 | 4 | 4 | 5 | 5 | 3 | 13 | 5 | 11 | 8 | 4 | 4 | 6 | 9 | 7 |

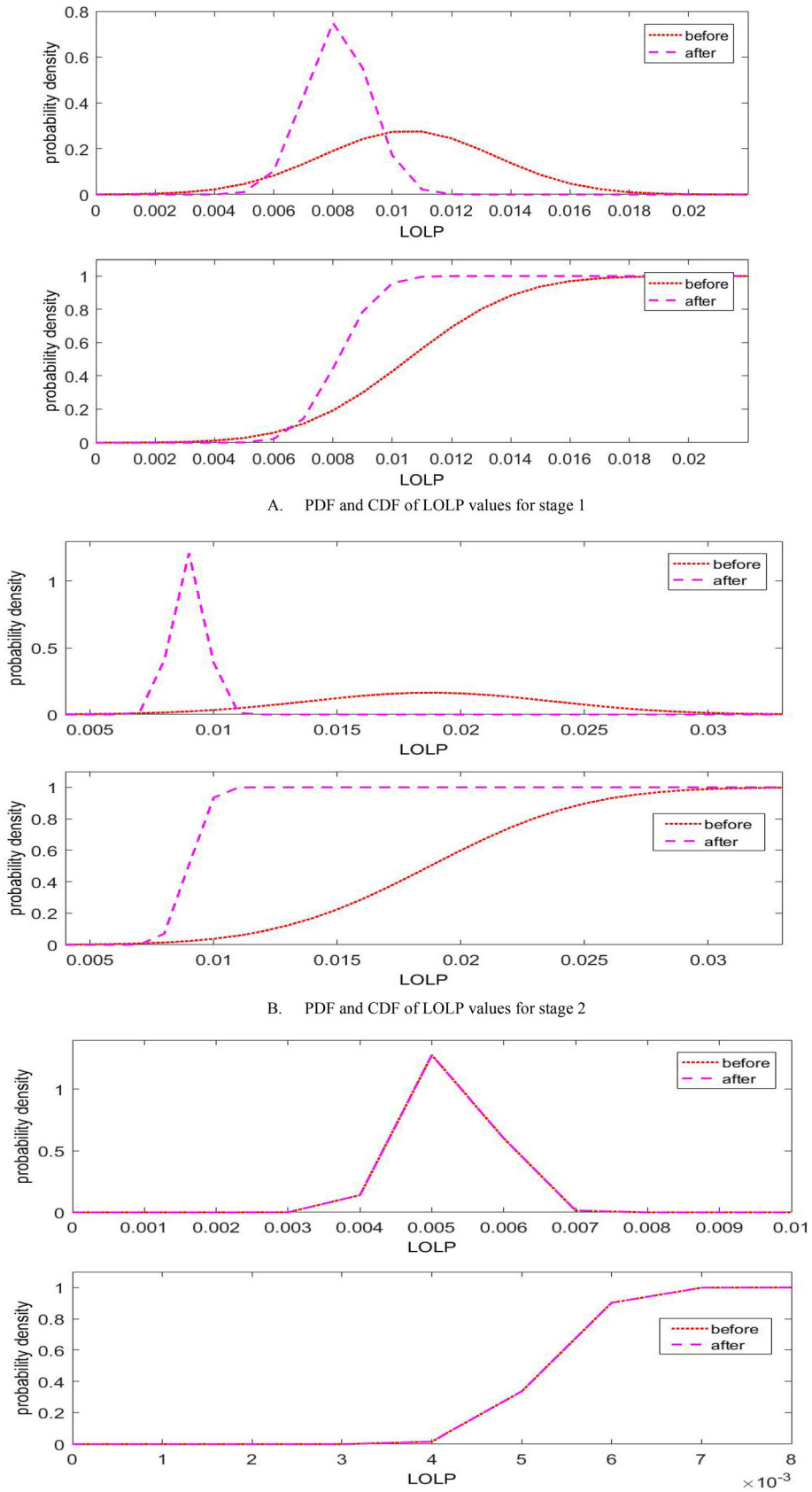


A. PDF and CDF of LOLP values for stage 1

B. PDF and CDF of LOLP values for stage 2

C. PDF and CDF of LOLP values for stage 6

**Fig. 16** PDF and CDF of LOLP values before and after adding capacity at 50% reserve capacity for policy 3-b

**Fig. 16** continued

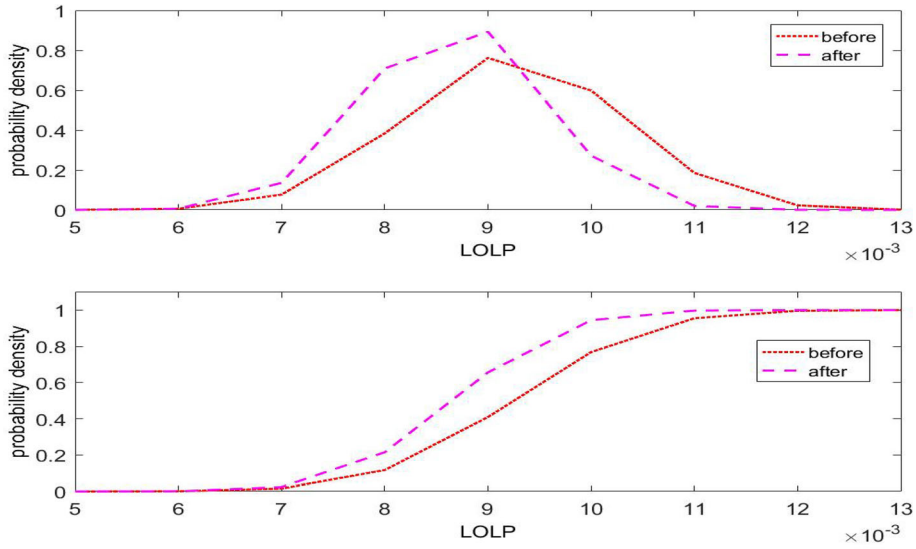


D. PDF and CDF of LOLP values for stage 9

#### 5.4.4 GEP results considering wind energy uncertainty for 12 stages case study

In this case of policy 3, for 12 stages (24 year planning horizon), the proposed HBA is utilized for solving the GEP problem at 50% and 60% reserve margin. The optimal results of the total number of newly candidate technology type are tabulated in Table 11. Also, FGT and PHS number units at each planning stage are recorded in the two columns Table 11, at different reserve margins. However, the PDF and CDF of LOLP values for this policy at 50% reserve margin for stages 1, 2, 6 and 9 are shown in Fig. 16. For stage 1, less than 40% of the scenarios are achieved all constraints before adding any units. On the other side, the LOLP values are achieved for all scenarios after adding one unit of FGT and one of PHS as shown in Fig. 16A. The number of addition units for stage 2 is more than respect to stage 1 because of the number of scenarios in stage 2, which achieved the constraints, is less than 10% of total scenarios as shown in Fig. 16B. In stages 3, 4, 5, 6,7, and 8, LOLP target is satisfied within the prescribed limit without any addition units which LOLP value is less than 0.01 as shown in Fig. 16C. Also, the LOLP constraint at stage 9 requires addting a nother FGT unit to achieve the target value. As shown in Fig. 16D, the required addition capacity is 150 MW of FGT because of 10% of the scenarios is infeasible of LOLP constraint. Considering the constraint of the reserve margin at 60%, the results of expansion planning is recorded in Table 11 where the LOLP values at stages a, 10 and 12 are displayed in Fig. 17. From Fig. 17A, less than 40% scenarios have LOLP value greater than the limit before adding one unit of FGT and one of PHS to correct this situation. More additional units are required at stage 10 to increase the LOLP value as shown in PDF and CDF in Fig. 17B. At stage 11, although no wind plant is deployed, the LOLP values are checked at the mean value of wind power scenarios, which penetrated in the previous stages, and has 0.089 value. Therefore, the LOLP target is achieved when checked with previous adding units at stage 11 while four FGT and three PHS units are required to adjust the LOLP value at stage 12.

#### 5.4.5 GEP Emission reduction strategy results considering wind energy uncertainty

The applications are extended to apply the proposed procedure on two test systems. Each system has two scenarios the first is based on the cost minimization while the second is based on the minimization of the emission. An assessment of the four scenarios is added. In addition to the previous four scenarios, the cost based scenario is implemented for large-scale test system. Tables 12 and 13 summarize the comparative 3-stages GEP model results obtained of two cases of objective functions at 60% reserve capacity margin for two cases that aimed at minimizing the total costs and minimizing the GHG emission in Cases 1 and 2, respectively. Similarly, Tables 14 and 15 summarize the comparative 6 stages GEP model results obtained of two cases of objective functions at 60% reserve capacity margin.

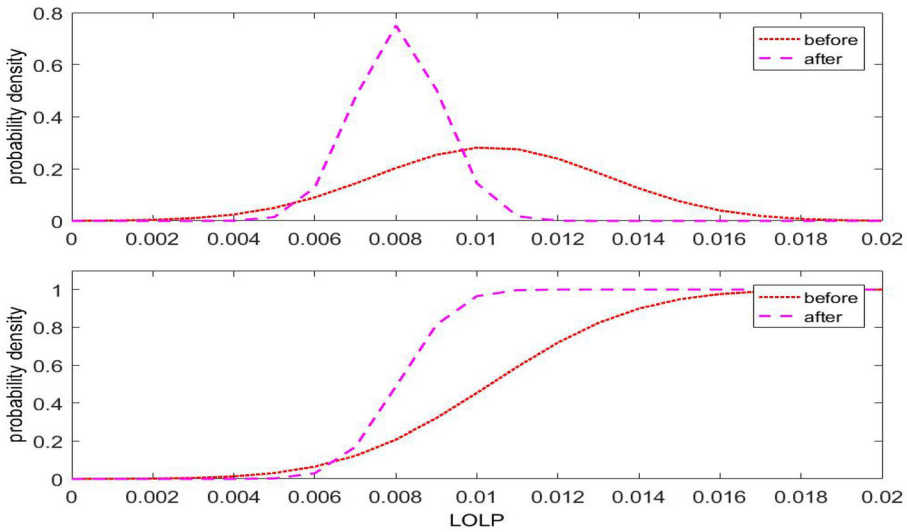


A. PDF and CDF of LOLP values for stage 1

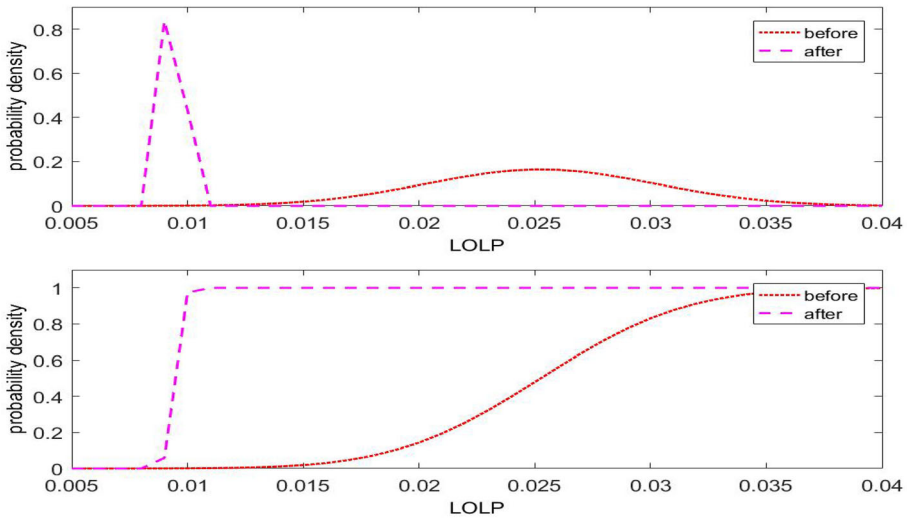


B. PDF and CDF of LOLP values for stage 10

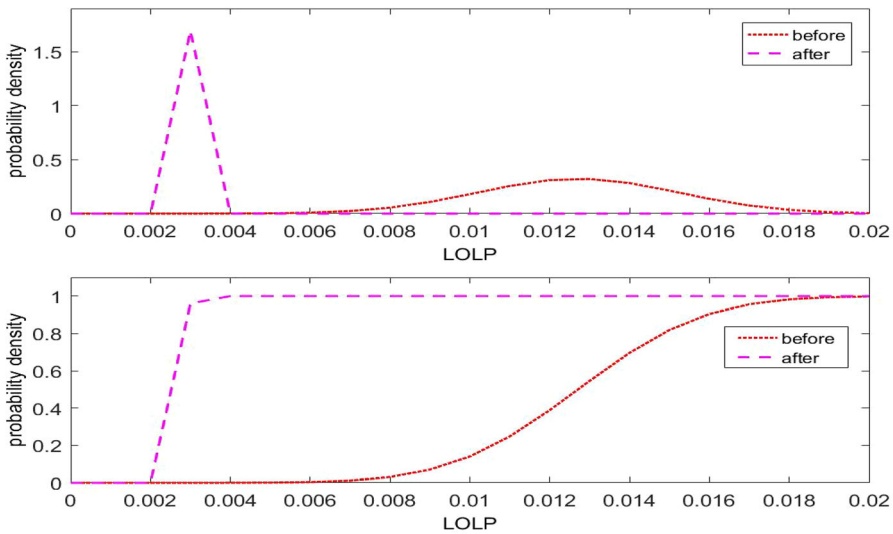


C. PDF and CDF of LOLP values for stage 12

**Fig. 17** PDF and CDF of LOLP values before and after adding capacity at 60% reserve capacity for policy 3-b

**Table 12** Comparative 3-stages GEP model results

| Objective function | Total cost $*10^9$ ($) | GHG emission$*10^3$ (Ton. $CO_2$) |
|---|---|---|
| Case 1: total Cost minimization | 8.21 | 5.4075 |
| Case 2: GHG emission minimization | 8.51 | 5.0525 |

**Table 13** Number of newly candidate units for 6 stages at 60% reserve Margin

| Stages | Oil | LNG | Coal | Nuclear #1 | Nuclear #2 | Wind (Zaf) | Wind (Shark) | FGT | PHS |
|---|---|---|---|---|---|---|---|---|---|
| 1 | 3 | 0 | 3 | 2 | 0 | 1 | 0 | 2 | 2 |
| 2 | 0 | 0 | 0 | 2 | 0 | 0 | 1 | 1 | 0 |
| 3 | 0 | 0 | 0 | 1 | 0 | 0 | 1 | 0 | 0 |
| Total | 3 | 0 | 3 | 5 | 0 | 1 | 2 | 3 | 2 |

**Table 14** Comparative 6 stages GEP model results

| Objective function | Total cost $*10^{10}$ ($) | GHG emission $*10^3$ (Ton. $CO_2$) |
|---|---|---|
| Case 1: total Cost minimization | 1.6665 | 8.4325 |
| Case 2: GHG emission minimization | 1.7603 | 7.8125 |

**Table 15** Number of newly candidate units for 6 stages at 60% reserve Margin

| Stages | Oil | LNG | Coal | Nuclear #1 | Nuclear #2 | Wind (Zaf) | Wind (Shark) | FGT | PHS |
|---|---|---|---|---|---|---|---|---|---|
| 1 | 3 | 3 | 2 | 2 | 0 | 0 | 1 | 0 | 0 |
| 2 | 0 | 0 | 2 | 2 | 0 | 0 | 1 | 0 | 0 |
| 3 | 0 | 0 | 0 | 0 | 1 | 0 | 0 | 0 | 0 |
| 4 | 0 | 1 | 1 | 0 | 2 | 1 | 0 | 0 | 0 |
| 5 | 0 | 0 | 0 | 1 | 0 | 0 | 1 | 0 | 0 |
| 6 | 3 | 0 | 1 | 0 | 0 | 1 | 0 | 0 | 0 |
| Total | 6 | 4 | 6 | 5 | 3 | 2 | 3 | 0 | 0 |

## 6 Conclusion

Reliability constrained GEP problem is a highly complex, nonlinear, multiple constraints and dynamic problem. Firstly, the GEP problem is solved without wind energy penetration and emission reduction constraint as the base case. The proposed HBA algorithm is applied with GEP model modifications to solve GEP problem and compared with other algorithms in the base case. Thus, the performance of the proposed HBA is better than other techniques. Also, reliability indies such as EENS and LOLP are calculated by ELDC as one of production simulation methods. The base case results indicate that the proposed HBA has effective and better performance than compared algorithms. Moreover, the robust GEP model as the short and long-term planning horizon is proposed in this paper and solved as the base case. Then, it is presented considering long and short-term wind uncertainties effect of the high share of wind energy from two different wind sites. Wind capacity credit from each wind site is considered during long-term uncertainty analysis as the first step. In the second step, wind power uncertainty from each site is modeled by wind speed scenarios based on its PDF and included in the planning by using MCS. For each scenario, all constraints are checked and addition capacities by FGT and/ or PHS units are added to deal with wind short-term uncertainty. The total costs are calculated in case of infeasible particles after adding penalty factor, and it calculated for feasible particles with wind scenarios after addition economic effect of the required capacities. The GEP models as reference case study and considering wind long and short-term uncertainties are analyzed for 3, 6, and 12 stages as short and long planning horizons. Simulation results indicated that considering wind long and short-term uncertainties in the expansion planning leads to a robust and flexible planning and guarantees the safe operation of system under uncertainty conditions. In the future work, the correlation factor between wind uncertainty scenarios and using other techniques for uncertainty analysis is suggested in the search space of the GEP problem with considering wind uncertainty. However, it is advised that the system's reliability be examined during the planning and operating phases to maintain it at target value, particularly when wind energy is penetrated. Additionally,

during the economic dispatch phase of the available generating units, the emission costs as an objective function should be taken into consideration. Also, the network-based GEP can be changed the problem complexity and therefore needs deep machine learning algorithms to handle the increased complexity.

**Funding** Open access funding provided by The Science, Technology & Innovation Funding Authority (STDF) in cooperation with The Egyptian Knowledge Bank (EKB).

**Data availability** Authors can confirm that all relevant data are included in the article.

## Declarations

**Conflict of interest** Authors have no conflict of interest in this work.



## References

1. Conejo AJ, Baringo L, Kazempour SJ, Siddiqui AS (2016) Investment in electricity generation and transmission. Springer International Publishing, Cham Zug, Switzerland
2. Shaheen AM, El-Sehiemy RA, Farrag SM (2016) A novel adequate bi-level reactive power planning strategy. Int J Electr Power Energy Syst 78:897–909. https://doi.org/10.1016/j.ijepes.2015.12.004
3. ELKARMI F (ed. ). (2012) Power system planning technologies and applications: concepts, solutions and management: concepts, solutions and management. IGI Global
4. Elattar EE, Shaheen AM, Elsayed AM, El-Sehiemy RA (2020) Optimal power flow with emerged technologies of voltage source converter stations in meshed power systems. IEEE Access. https://doi.org/10.1109/access.2020.3022919
5. El-Ela AAA, Bishr M, Allam S, El-Sehiemy R (2005) Optimal preventive control actions using multi-objective fuzzy linear programming technique. Electr Power Syst Res 74:147–155. https://doi.org/10.1016/j.epsr.2004.08.014
6. El-Sehiemy RA, El Ela AAA, Shaheen A (2015) A multi-objective fuzzy-based procedure for reactive power-based preventive emergency strategy. Int J Eng Res Africa 13:91–102. https://doi.org/10.4028/www.scientific.net/JERA.13.91
7. Babatunde BOM, Munda JL, Hamam Y (2019) A comprehensive state-of-the-art survey on power generation expansion planning with intermittent renewable energy source and energy storage. Int J Energy Res 43(12):6078–6107. https://doi.org/10.1002/er.4388
8. Quan H, Khosravi A, Yang D (2019) A survey of computational intelligence techniques for wind power uncertainty quantification in smart grids. IEEE Trans Neural Netw Learn Syst 31:4582–4599. https://doi.org/10.1109/TNNLS.2019.2956195
9. Jordehi AR (2018) How to deal with uncertainties in electric power systems? A review. Renew Sustain Energy Rev 96:145–155. https://doi.org/10.1016/j.rser.2018.07.056
10. MANSOURI, Seyed Amir; JAVADI MS, (2017) A robust optimisation framework in composite generation and transmission expansion planning considering inherent uncertainties. J Exp Theor Artif Intell 29:717–730. https://doi.org/10.1080/0952813X.2016.1259262
11. Guo J, Fang Y, Kawamoto E, et al (2022) A review of hydrogen-based hybrid renewable energy systems: Simulation and optimization with artificial intelligence A review of hydrogen-based hybrid renewable energy systems: Simulation and optimization with artificial intelligence. https://doi.org/10.1088/1742-6596/2208/1/012012
12. Ali ES, El-Sehiemy RA, Abou El-Ela AA (2021) Optimal partitioning of unbalanced active distribution systems for supply-sufficient micro-grids considering uncertainty. Int Transact Electr Energy Syst 31(12):e13210. https://doi.org/10.1002/2050-7038.13210
13. Akbarzade, Hossein and Amraee T (2018) A Model for Generation Expansion Planning in Power Systems Considering Emission Costs. In: 2018 Smart Grid Conf (SGC), IEEE 1–5. https://doi.org/10.1109/SGC.2018.8777836
14. JADIDOLESLAM, Morteza; EBRAHIMI A, (2015) Reliability constrained generation expansion planning by a modified shuffled frog leaping algorithm. Int J Electr Power Energy Syst 64:743–751. https://doi.org/10.1016/j.ijepes.2014.07.073
15. Pereira S, Ferreira P, Vaz AIF (2016) Optimization modeling to support renewables integration in power systems. Renew Sustain Energy Rev 55:316–325. https://doi.org/10.1016/j.rser.2015.10.116
16. Abou El-Ela AA, El-Sehiemy RA, Ali ES, Kinawy A-M (2019) Minimisation of voltage fluctuation resulted from renewable energy sources uncertainty in distribution systems. IET Gener Transm Distrib 13:2339–2351. https://doi.org/10.1049/iet-gtd.2018.5136
17. Jadidoleslam M, Bijami E, Amiri N, Ebrahimi A (2012) Application of shuffled frog leaping algorithm to long term generation expansion planning. Int J Comput Electr Eng 4:115
18. Kannan S, Baskar S, McCalley JD, Murugan P (2008) Application of NSGA-II algorithm to generation expansion planning. IEEE Trans Power Syst 24:454–461
19. Rashidaee SA, Amraee T, Fotuhi-Firuzabad M (2018) A linear model for dynamic generation expansion planning considering loss of load probability. IEEE Trans Power Syst 33:6924–6934. https://doi.org/10.1109/TPWRS.2018.2850822
20. Park H, Baldick R (2015) Stochastic generation capacity expansion planning reducing greenhouse gas emissions. IEEE Trans Power Syst 30:1026–1034
21. Bhuvanesh A, Christa J, Thomas S, Kannan S, Karuppasamy Pandiyan M (2019) Multistage multiobjective electricity generation expansion planning for Tamil Nadu considering least cost and minimal GHG emission. Int Trans Electr Energy Syst 29:e2708. https://doi.org/10.1002/etep.2708
22. Javadi MS, Esmaeel NA (2019) Multi-objective, multi-year dynamic generation and transmission expansion planning-renewable energy sources integration for Iran's national power grid. Int Transact Electr Energy Syst 29(4):e2810. https://doi.org/10.1002/etep.2810
23. Kannan S, Slochanal SM, Subbaraj P, Padhy NP (2004) Application of particle swarm optimization technique and its variants

to generation expansion planning problem. Electr Power Syst Res 70(3):203–210. https://doi.org/10.1016/j.epsr.2003.12.009
24. Karunanithi K, Kannan S, Thangaraj C (2015) Generation expansion planning for Tamil Nadu: a case study. Int Trans Electr energy Syst 25:1771–1787. https://doi.org/10.1002/etep
25. Pereira AJ, Saraiva JT (2010) A decision support system for generation expansion planning in competitive electricity markets. Electr power Syst Res 80(778):787. https://doi.org/10.1016/j.epsr.2009.12.003
26. Hemmati R, Hooshmand R-A, Khodabakhshian A (2013) Reliability constrained generation expansion planning with consideration of wind farms uncertainties in deregulated electricity market. Energy Convers Manag 76:517–526. https://doi.org/10.1016/j.enconman.2013.08.002
27. Hemmati R, Hooshmand R, Khodabakhshian A (2016) Coordinated generation and transmission expansion planning in deregulated electricity market considering wind farms. Renew Energy 85:620–630. https://doi.org/10.1016/j.renene.2015.07.019
28. SAXENA, Kritika; BHAKAR, Rohit; JAIN P (2018) Coordinated GEP and TEP Approach with Correlated Generation and Load. In: 2018 3rd Int Conf Work Recent Adv Innov Eng 1–6
29. Hemmati R, Hooshmand R, Khodabakhshian A (2014) Market based transmission expansion and reactive power planning with consideration of wind and load uncertainties. Renew Sustain Energy Rev 29:1–10. https://doi.org/10.1016/j.rser.2013.08.062
30. Alaee S, Hooshmand RA, Hemmati R (2016) Stochastic transmission expansion planning incorporating reliability solved using SFLA meta-heuristic optimization technique. CSEE J Power Energy Syst 2(2):79–86. https://doi.org/10.17775/CSEEJPES.2016.00025
31. Hochreiter S (1997) Long short-term memory. Neural Comput 9:1735–1780
32. Skrobek D, Krzywanski J, Sosnowski M, Kulakowska A, Zylka A, Grabowska K, Ciesielska K, Nowak W (2022) Implementation of deep learning methods in prediction of adsorption processes. Adv Eng Softw 173:103190. https://doi.org/10.1016/j.advengsoft.2022.103190
33. ABDALLA, Omar H.; ADMA, Maged A. Abu; AHMED AS (2019) Generation Expansion Planning Considering High Share Renewable Energies Uncertainty. In: 2019 21st Int Middle East Power Syst Conf (MEPCON) IEEE 1–7
34. Abdalla OH, Adma MAA, Ahmed AS (2020) Generation expansion planning under correlated uncertainty of mass penetration renewable energy sources. IET ENERGY Syst Integr 2:273–281. https://doi.org/10.1049/iet-esi.2020.0008
35. Abdalla OH, Smieee L, Adma MAA, Ahmed AS (2020) Two-stage robust generation expansion planning considering long- and short-term uncertainties of high share wind energy. Electr Power Syst Res 189:106618. https://doi.org/10.1016/j.epsr.2020.106618
36. Kumar PP, Nuvvula RSS, Hossain A, Shezan SKA (2022) Optimal operation of an integrated hybrid renewable energy system with demand-side management in a rural context. Energies 15:5176
37. Hossen MD, Islam MF, Ishraque MF, Shezan SA, Arifuzzaman SM (2022) Design and implementation of a hybrid solar-wind-biomass renewable energy system considering meteorological conditions with the power system performances. Int J Photoenergy 2:2022
38. Shezan SA, Ishraque F, Muyeen SM et al (2022) Selection of the best dispatch strategy considering techno-economic and system stability analysis with optimal sizing. Energy Strateg Rev 43:100923. https://doi.org/10.1016/j.esr.2022.100923
39. Shezan SA, Ishraque F, Muyeen SM et al (2022) Effective dispatch strategies assortment according to the effect of the operation for an islanded hybrid microgrid. Energy Convers Manag X 14:100192. https://doi.org/10.1016/j.ecmx.2022.100192
40. Shezan SA, Ishraque MF, Paul LC, Sarkar MR, Rana MM, Uddin M, Hossain MB, Shobug MA, Hossain MI (2022) Assortment of dispatch strategies with the optimization of an islanded hybrid microgrid. MIST Int J Sci Technol 26(10):15–24
41. Farh HMH, Al-shamma AA, Al-shaalan AM, Alkuhayli A (2022) Technical and economic evaluation for off-grid hybrid renewable energy system using novel bonobo optimizer. Sustainability 14:1533
42. Xifan, Wang and McDonald JR (1994) Modern power system planning. 208–229
43. Choi J, Lee KY (2021) Probabilistic power system expansion planning with renewable energy resources and energy storage systems. Wiley
44. RASHIDAEE, Seyyed Ali; AMRAEE T (2018) Generation Expansion Planning Considering the Uncertainty of Yearly Peak Important Deadlines for Technical Papers. In: Eng 2018 IEEE Ind Commer Power Syst Eur (EEEIC/I&CPS Eur IEEE 1–4. https://doi.org/10.1109/EEEIC.2018.8493688
45. Barati F, Jadid S, Zangeneh A (2019) Private investor-based distributed generation expansion planning considering uncertainties of renewable generations. Energy 15(173):1078–1091. https://doi.org/10.1016/j.energy.2019.02.086
46. Pereira S, Ferreira P, Vaz AIF (2017) Generation expansion planning with high share of renewables of variable output. Appl Energy 190:1275–1288. https://doi.org/10.1016/j.apenergy.2017.01.025
47. Abdalla OH, Abu Adma MA, Ahmed AS (2021) Generation expansion planning considering unit commitment constraints and data-driven robust optimization under uncertainties. Int Transact Electr Energy Syst 31(6):e12878. https://doi.org/10.1002/2050-7038.12878
48. Muppidi R, Nuvvula RS, Muyeen SM, Shezan SA, Ishraque MF (2022) Optimization of a fuel cost and enrichment of line loadability for a transmission system by using rapid voltage stability index and grey wolf algorithm technique. Sustainability 14(7):4347. https://doi.org/10.3390/SU14074347
49. Nawaz U (2020) Least-cost generation expansion planning using whale optimization algorithm incorporating emission reduction and renewable energy sources. Int Trans Electr Energy Syst 30:e12238. https://doi.org/10.1002/2050-7038.12238
50. Rajesh K, Kannan S, Thangaraj C (2016) Least cost generation expansion planning with wind power plant incorporating emission using differential evolution algorithm. Int J Electr power energy Syst 80:275–286. https://doi.org/10.1016/j.ijepes.2016.01.047
51. Rajesh K, Bhuvanesh A, Kannan S, Thangaraj C (2016) Least cost generation expansion planning with solar power plant using differential evolution algorithm. Renew Energy 85:677–686. https://doi.org/10.1016/j.renene.2015.07.026
52. Rajesh K, Karthikeyan K, Kannan S, Thangaraj C (2016) Generation expansion planning based on solar plants with storage. Renew Sustain Energy Rev 57:953–964. https://doi.org/10.1016/j.rser.2015.12.126
53. Booma J, Mahadevan K, Kannan S (2015) Minimum cost estimation of generation expansion planning incorporating wind power plant. ARPN J Eng Appl Sci 10:2956–2961
54. SEIFI, Hossein; SEPASIAN MS, (2011) Electric power system planning: issues, algorithms and solutions. Springer, Berlin
55. Billington, Roy and Allan RN (1994) Reliability Evaluation of Power Systems
56. Shaheen AM, Elattar EE, El RA et al (2020) An improved sunflower optimization algorithm based-Monte Carlo simulation for efficiency improvement of radial distribution systems considering wind power uncertainty. IEEE Access 9:2332–2344. https://doi.org/10.1109/ACCESS.2020.3047671

57. El-Ela A, Abou El-Ela AA, El-Sehiemy RA et al (2022) Renewable Energy micro-grid interfacing: economic and environmental issues. Electronics. https://doi.org/10.3390/electronics11050815
58. Shaheen AM, Ginidi AR, El-Sehiemy RA, Elattar EE (2021) Optimal economic power and heat dispatch in cogeneration Systems including wind power. Energy 225:120263. https://doi.org/10.1016/j.energy.2021.120263
59. Akdağ SAGÖ (2011) A comparison of wind turbine power curve models. Energy Sources, Part A Recover Util Environ Eff 33:2257–2263. https://doi.org/10.1080/15567036.2011.594861
60. Hashim FA, Houssein EH, Hussain K, Mabrouk MS, Al-Atabany W (2022) Honey badger algorithm: new metaheuristic algorithm for solving optimization problems. Math Comput Simul 192:84–110. https://doi.org/10.1016/j.matcom.2021.08.013
61. Nawaz U, Malik TN, Ashraf MM (2020) Least-cost generation expansion planning using whale optimization algorithm incorporating emission reduction and renewable energy sources. Int Transact Electr Energy Syst 30(3):e12238. https://doi.org/10.1002/2050-7038.12238
62. Rajesh K, Bhuvanesh A, Kannan S, Thangaraj C (2022) Least cost generation expansion planning with solar power plant using differential evolution algorithm. Renew Energy 85:677–686. https://doi.org/10.1016/j.renene.2015.07.026
63. Askarzadeh A (2016) A novel metaheuristic method for solving constrained engineering optimization problems: crow search algorithm. Comput Struct. https://doi.org/10.1016/j.compstruc.2016.03.001
64. Abualigah L, Yousri D, Abd Elaziz M, Ewees AA, Al-Qaness MA, Gandomi AH (2021) Aquila optimizer: a novel meta-heuristic optimization algorithm. Comput Ind Eng 1(157):107250. https://doi.org/10.1016/j.cie.2021.107250
65. Alsattar HA, Zaidan AA, Zaidan BB (2020) Novel meta-heuristic bald eagle search optimisation algorithm. Artif Intell Rev. https://doi.org/10.1007/s10462-019-09732-5
66. Abou El-Ela AA, El-Sehiemy RA, Shaheen AM, Shalaby AS (2023) Assessment of Wind Energy based on Optimal Weibull Parameters Estimation using Bald Eagle Search Algorithm: Case Studies from Egypt. J Electr Eng Technol 18:4061–4078. https://doi.org/10.1007/s42835-023-01492-1